ESTABLISHING DEGRADATION RATES AND SERVICE LIFETIME OF PHOTOVOLTAIC SYSTEMS

by

ALBERT LEYTE-VIDAL
B.S. University of Central Florida, 2008

A thesis submitted in partial fulfillment of the requirements
for the degree of Master of Science
in the Department of Electrical Engineering
in the college of Engineering and Computer Science
at the University of Central Florida
Orlando, Florida

Summer Term
2010

ABSTRACT

As fossil fuel sources continue to diminish, oil prices continue to increase, and global warming and CO_2 emissions keep impacting the environment, it has been necessary to shift energy consumption and generation to a different path. Solar energy has proven to be one of the most promising sources of renewable energy because it is environmentally friendly, available anywhere in the world, and cost competitive.

For photovoltaic (PV) system engineers, designing a PV system is not an easy task. Research demonstrates that different PV technologies behave differently under certain conditions; therefore energy production varies not only with capacity of the system but also with the type of module. For years, researchers have also studied how these different technologies perform for long periods of time, when exposed out in the field.

In this study, data collected by the Florida Solar Energy Center for periods of over four years was analyzed using two techniques, widely accepted by researchers and industry, to evaluate the long-term performance of five systems. The performance ratio analysis normalizes system capacity and enables the comparison of performance between multiple systems. In PVUSA Regression analysis, regression coefficients are calculated which correspond to the effect of irradiance, wind speed, and ambient temperature, and these coefficients are then used to calculate power at a predetermined set of conditions.

This study allows manufacturers to address the difficulties found on system lifetime when their modules are installed out on the field. Also allows for the further development and improvement of the different PV technologies already commercially available.

ACKNOWLEDGMENTS

Several people have been of invaluable support to me during the last eighteen months of conducting this research and writing this thesis. First of all, I'd like to thank my supervisor, Dr. Nicoleta Sorloacia-Hickman, for giving me the opportunity to be part of her research group at the Florida Solar Energy Center (FSEC), and Dr. James Hickman for being my advisor and guiding me when I needed it.

I'd like to also thank Kris Davis, Houtan Moaveni, William Wilson, and Steven Nason, for their continuous support and help. Since day one these people were always available and willing to answer any of my questions regarding anything related to this research. I can't forget to mention Mr. Scott Reinhart and the rest of the staff from FSEC, who were always there when I needed them.

Finally, I'd like to thank Dr. Sarah Kurtz and Dirk Jordan from the National Renewable Energy Laboratory (NREL) for their ideas and encouragement. Their ideas and experience helped me accomplish what needed to be accomplished for this project.

I have been very fortunate to work surrounded by a very helpful and friendly group of people. It has been a great time the past eighteen months, and I have surely learned a lot from this experience.

TABLE OF CONTENTS

LIST OF FIGURES

LIST OF TABLES

NOMENCLATURE

Abbreviation	Definition
AC	Alternating Current
AM	Air Mass
a-Si	Amorphous Silicon
DAS	Data Acquisition System
DC	Direct Current
FSEC	Florida Solar Energy Center
IEC	International Electrotechnical Commission
I_{mp}	Maximum Power Current
I_{sc}	Short Circuit Current
I-V	Current-Voltage
MER	Module Energy Rating
m-Si	Mono Crystalline
NEC	National Electric Code
NREL	National Renewable Energy Lab
P_{max}	Maximum Power
p-n	p-type & n-type semiconductor junction
p-Si	Poly Crystalline
PR	Performance Ratio
PTC	PVUSA Testing Conditions
PV	Photovoltaic
PVUSA	Photovoltaics for Utility Scale Applications
R&D	Research & Development
SAM	Solar Advisor Model
SDA	System-Drive Approach
STC	Standard Test Conditions
TMY	Typical Meteorological Year
V_{oc}	Open Circuit Voltage
V_{mp}	Maximum Power Voltage
α	Temperature Coefficient for Short Circuit Current
β	Temperature Coefficient for Open Circuit Voltage
γ	Temperature Coefficient for Max Power

CHAPTER 1 INTRODUCTION

1.1 Background

Developing clean and renewable energy has become one of the most important tasks assigned to modern science and engineering. Photovoltaic (PV) energy looks to be a very promising future energy resource as it is pollution free and abundantly available anywhere in the world. It is cost-effective for remote applications where utility power is unavailable, and in many parts of the world, it is becoming cost-competitive with traditional sources of utility power (e.g. Germany, Japan, California).

It is important to conduct accurate and dependable studies of PV system performance for the future development of these systems. For different manufacturers, analysis and performance assessment is a benchmark of quality for existing products and a help to reevaluate product warranty and long term performance. For the research and development community (R&D), these studies are an aid to identify future needs. Finally, for system integrators and end-users, they are a guide to evaluate product quality and a help in decision-making. However, in the past, less effort has been placed to validate models using PV systems installed in the field over long periods of time. The performance characteristics of PV modules are needed in order to model their annual performance [1][2].

As the industry grows, a clear need is rising for greater education about appropriate industry-standard performance parameters for PV systems. Performance parameters allow for the detection of operational problems, facilitate the comparison of systems that

may differ with respect to design, technology, or geographical location, and validate models for system performance estimation during the design phase. Industry-wide use of standard performance parameters and system ratings will assist investors in evaluating different proposals and technologies, giving them greater confidence in their own ability to procure and maintain reliable, high-quality technologies. Standard methods of evaluation and rating will also help to set appropriate expectations for performance with educated customers, ultimately leading to increased credibility for the PV industry and positioning it for further growth.

Solar PV's are arrays of cells containing a material that converts solar radiation into direct current (DC) electricity [3]. Module degradation and failure is often present in PV systems but not immediately recognized. System design can frequently mask the effects of module performance degradation and/or individual module failures. On the other hand, some module degradation mechanisms can significantly degrade the operation and/or performance of the entire system. This is why identifying degradation mechanisms and establishing degradation rates has become significantly important in this industry.

Information on system performance at different locations has been remotely collected since the 1990's at the Florida Solar Energy Center (FSEC). However, lack of support has impeded coordination of such data, resulting in minimal data being generated with varied measurement techniques and analytical methods. Therefore, there is opportunity to better utilize this data toward understanding degradation rates and PV performance.

1.2 Objectives of the Thesis

The overall objective of this thesis is to provide a comprehensive analysis of the degradation rates and the performance characteristics of a variety of field-aged PV systems installed in the state of Florida, while providing a basis for their assessment and developing practical recommendations. This project focuses on utilizing an existing PV database at the Florida Solar Energy Center, containing remotely collected data such as DC Voltage, DC Current, AC Power and ambient temperature at various systems and locations to validate the energy rating models.

This objective is achieved by using data collected and monitored by FSEC for the last 15 years, and comparing the output of several PV systems by applying different techniques. The recorded data is used to see how different PV performance prediction methods are able to predict the power output of all the different technologies.

1.3 Thesis Outline

This study compares the degradation rates found in five different PV systems installed in the state of Florida. Weather and module data collected for several years contribute to the development of this study by providing the data necessary to estimate performance of these systems.

Chapter two presents the research and information necessary in order to understand the analysis performed on the collected data. First, an introduction to PV is presented followed by background information on standard methods of rating PV modules and systems. Also, an introduction to mathematical models such as the Simple-Energy

Flow model and the One-Diode Solar Cell Model is presented in this section along with the research and information necessary to analyze the performance of the systems.

Chapter three presents an overview of PV module testing and monitoring. It includes a brief description of FSEC's PV Module Testing and Characterization Facility, an overview of outdoor measurements, and a description of outdoor testing facility. A discussion of the instrumentation used to collect meteorological and PV system performance data is presented at the end of the chapter.

Chapter four presents the long-term evaluation of the systems and their performance. A brief description of how the data is acquired, how the data is divided into months and filtered is also presented, followed by the results obtained by performing the different analyses. The end of chapter four presents a study relating theoretical and experimental performance of PV panels as function of angle of incidence and installation angle.

Finally, chapter five presents a summary of the results obtained in the form of a conclusion accompanied by suggestions and future work to be performed.

CHAPTER 2 PV MODULES AND PV MODELS

2.1 Introduction

PV arrays are composed of multiple PV modules comprised of numerous cells that convert incident light into electrical power through utilization of the photoelectric effect. The basic energy flow of a grid-tied PV system begins with the generation of DC electricity by an array of PV modules. PV cells are connected electrically in a PV module and they are the primary source of power in a PV system feeding an electrical load as show in Figure 2-1.

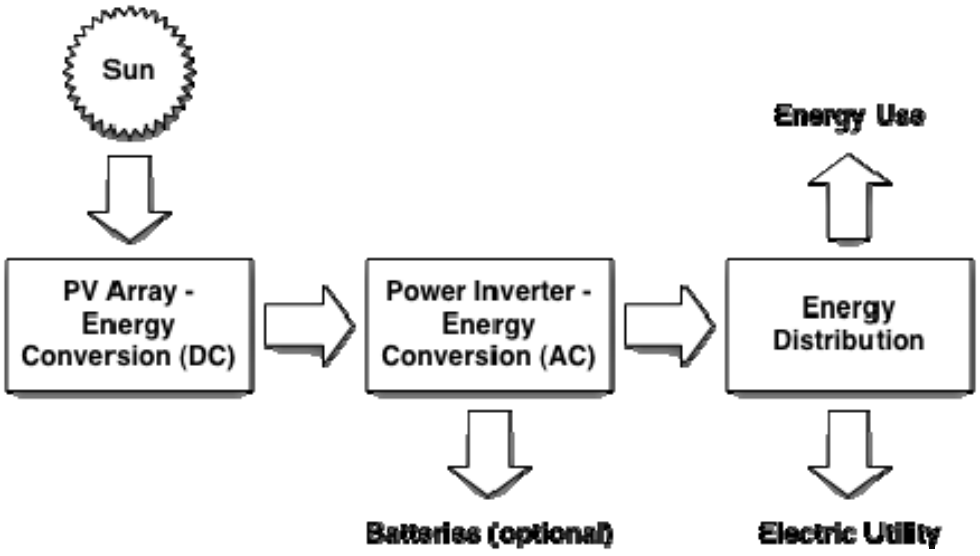

Figure 2-1 PV System Energy Flow

There are several types of PV technologies commercially available, but the most popular today are monocrystalline Silicon (m-Si), polycrystalline Silicon (p-Si), amorphous Silicon (a-Si), and Cadmium Telluride (CdTe) modules. As their name state, m-Si and p-Si are crystalline materials, but a-Si and CdTe are thin film materials. All these materials vary from each other in terms of light absorption efficiency, energy conversion efficiency,

manufacturing technology and cost of production [33]. Figure 2-2 below represents the current production share for the most common PV technologies.

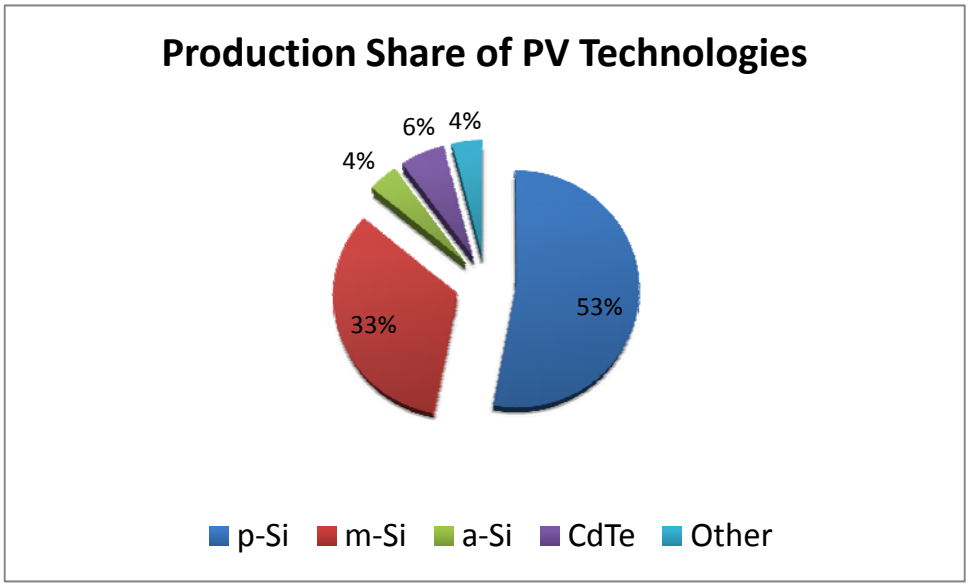

Figure 2-2 Current Production Share of PV Technologies [34]

In a grid-tied system, the array is coupled with an inverter, which converts the DC power produced into AC power. The inverter acts as the interface between the PV array and both the on-site loads and the electric utility. This allows the DC power generated by the modules to be both consumed by AC loads on-site and also to be exported back to the grid when the PV system is generating more power than the building is consuming.

On the other hand, not all PV systems are grid-connected. Some systems are remotely installed where a utility grid is not available and batteries must be installed to store energy. Batteries store electrical energy when it is produced by the array and supply energy to electrical loads when needed [4].

Finally, energy production in a PV system is directly proportional to the amount of solar irradiance incident on the array, which is dictated by both the tilt angle of the

modules with respect to the earth's surface and the directional orientation of the array. Also as seasons fluctuate throughout the year, the incidence angle fluctuates for a given location. Figure 2-3 demonstrates this effect for a Central Florida location.

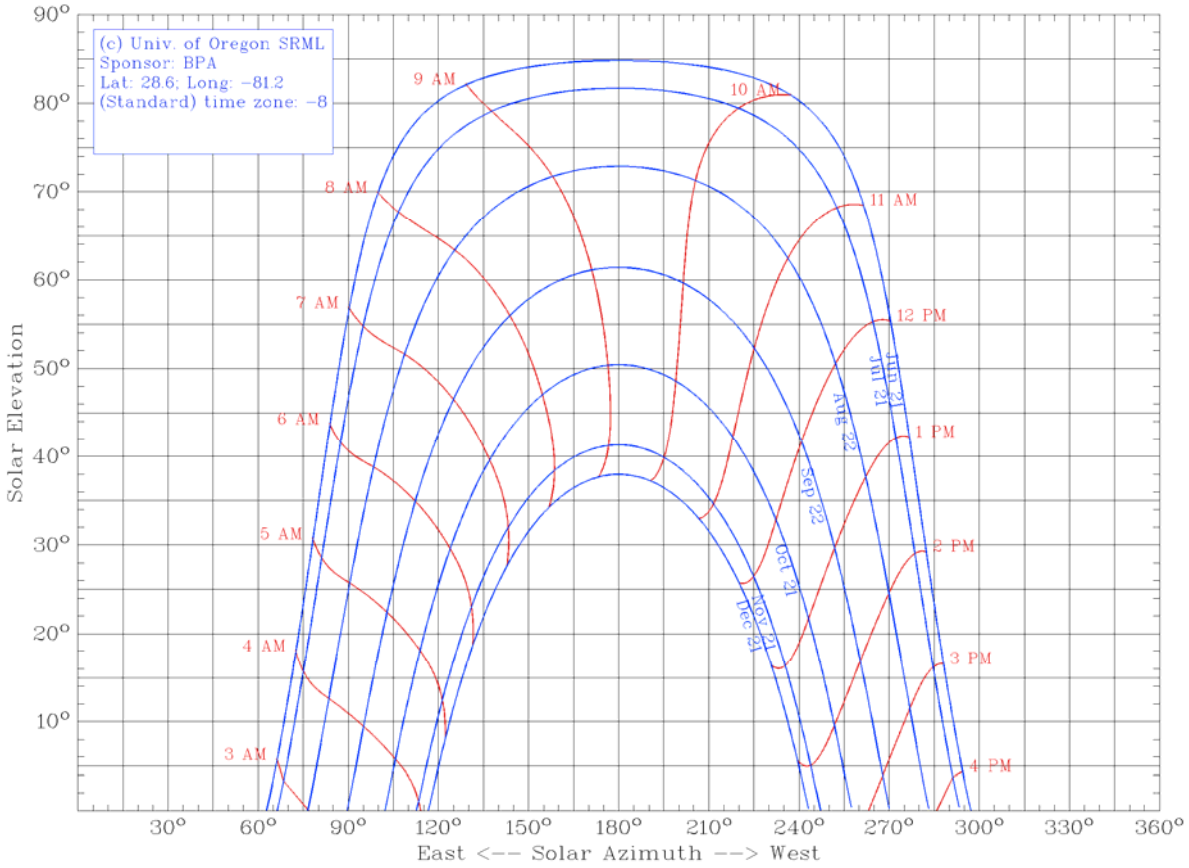

Figure 2-3 Solar Window [5]

2.2 Standard Performance Rating for PV Modules

Since 1906, the International Electrotechnical Commission (IEC) has been developing, interpreting, and maintaining standards in order to promote international uniformity in the field. In 2005 and 2008, IEC published the second edition of IEC

standards 61215 and 61646, to address the proper testing techniques of crystalline silicon photovoltaic modules and thin-film photovoltaic modules, respectively.

The electrical performance of solar modules varies depending on mostly on the irradiance and the temperature at which they operate. In order to keep uniformity in the measurements and specifications and to give a fair comparison between different products, Standard Test Conditions (STC) as described by the IEC must be followed when determining maximum power generation capacity, implying that the modules must be kept at 25°C and trace is current-voltage (I-V) characteristics at an irradiance of 1,000 W/m^2 with an air mass of AM1.5G, using natural sunlight or a class B or better simulator for crystalline modules [6], and a class BBB or better simulator for thin-film modules [7] Air mass is simply the distance the sun light has to travel in order to reach the Earth's surface. When the sun is perpendicular to the Earth's surface, sunlight only has to pass through the air mass (AM) of the atmosphere once. On the other hand, sun located at $\Theta = 30°$ above the horizon represents AM2 [37]. Equation 2-1 is used to calculate air mass with respect to sun elevation with respect to the horizon.

$$AM = 1/Sin(\theta) \qquad (2\text{-}1)$$

Based on Article 690 of the National Electric Code [32], PV manufacturers must have the following parameters listed on their modules:

P_{max} - Maximum Power Rated

V_{oc} - Open Circuit Voltage

I_{sc} - Short Circuit Current

V_{mp} - Maximum Power Voltage

I_{mp} - Maximum Power Current

Other type of information also provided may include temperature coefficients, which help relate the current, voltage, and power behavior according the module temperature.

2.3 Indoor and Outdoor Testing of PV Modules

Outdoor testing consists of installing a module, or array of modules, and collecting electrical performance data and weather data over a certain period of time. Testing for the STC power rating is normally done in accordance with IEC standards 61215 or 61646 (61215 for crystalline silicon, 61646 for thin film), or other established standards like ASTM E1036 or UL 1703. On the other hand, outdoor testing can also include the study of long-term performance under natural weather conditions. Because the environment cannot be controlled, outdoor testing is an excellent way to examine how PV modules behave when they are performing out in the field.

Indoor testing of photovoltaic modules allows examining modules under accelerated conditions if needed. Testing of crystalline modules require that a Class B solar simulator is used, while thin-film modules require that Class BBB simulators are used, as stipulated on IEC standards 61215 and 61646 respectively, or as stated in ATM E1036E or UL 1703 standards. NREL's High-Bay Accelerated Testing Laboratory is equipped with instruments that can be used to weather PV modules in environments with controlled temperature, ultraviolet exposure, and relative humidity [31].

2.4 PV Models and Simulation Tools

Some mathematical equations and models help engineers and researchers model the different characteristics and behaviors of solar cells. The Simple Energy Flow Model allows determining the power to be produced by a solar cell or array, at a given irradiance and temperature using manufacturer or calculated temperature coefficients. On the other hand, the One-Diode Solar Cell Model allows modeling mathematically the behavior of the I-V curve of a solar cell.

2.4.1 Simple Energy Flow Model

Temperature coefficients provide the rate of change (derivative) with respect to temperature of different photovoltaic performance parameters [8]. Measurements should take place in an environment where the total irradiance is at least as high as the upper limit of the range of interest, the irradiance variation caused by short-term oscillations is less than ±2% of the total irradiance as measured by the reference device, and the wind speed is less than 2 m/s [6][7]. Three coefficients are calculated by plotting the measured values for short-circuit current I_{sc}, open-circuit voltage V_{oc}, and maximum power P_{mp}, as functions of module temperature, and fitting a straight line. The calculated slopes of the regression correspond for the coefficient values of α , β, and γ for I_{sc}, V_{oc}, and P_{mp}, respectively. By applying equation 2-2, the maximum power can be estimated at certain conditions,

$$P = P_{REF}\left(\frac{IRR}{IRR_{REF}}\right)[1 + \gamma(T_{mod} - T_{modREF})] \qquad (2.2)$$

where,

P_{REF} - Reference Power at STC (W)

IRR - Measured Irradiance (W/m^2)

IRR_{REF} - Reference Irradiance (1000 W/m^2)

γ - Temperature Coefficient for Max Power

T_{mod} - Temperature of Module

T_{modREF} - Reference Module Temperature (25 C)

Table 2-1 below represents what this method of correcting the data can do. The value used for the temperature coefficient of the modules composing this array was chosen to be -0.485%/°C.

Table 2-1 Measured and Corrected Data

	IRR (W/m^2)	T_{mod} (°C)	$P_{measured}$ (W)	$P_{corrected}$ (W)
Measurement 1	1056	52.3	1620.2	1814.1
Measurement 2	1060	52.4	1626.2	1819.9
Measurement 3	1074	56.2	1610.1	1804.7

2.4.2 One Diode Solar Cell Model

A solar cell is basically a p-n semiconductor junction that when exposed to light, current proportional to solar irradiance is generated [21]. The equivalent circuit is shown in Figure 2-4 below.

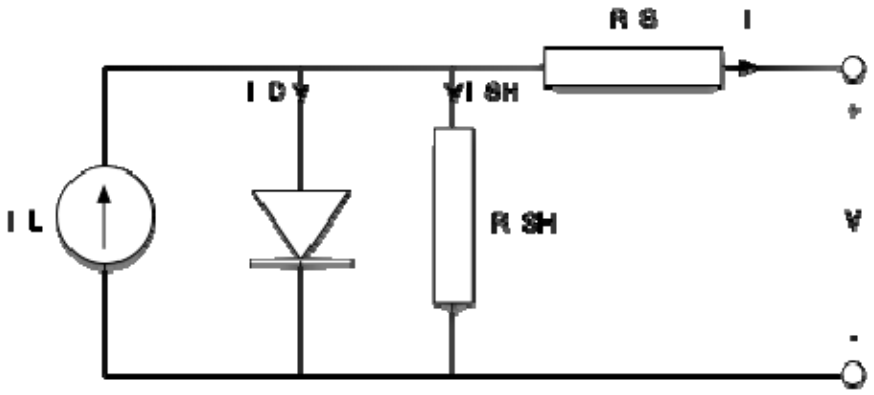

Figure 2-4 One Diode Solar Cell Model

The mathematical expressions that describe the I-V curve characteristics of this model are [21]:

$$I_D = I_o\left(e^{\frac{q(V+IR_S)}{kT}} - 1\right) \qquad (2\text{-}3)$$

$$I = I_L - I_D - V + \frac{IR_S}{R_{SH}} \qquad (2\text{-}4)$$

where,

I - Cell Current (A)

q - Charge of Electron (1.6×10^{-9} coulombs)

k - Boltzmann Constant (1.38×10^{-23} m^2kg/s^2K)

T - Cell Temperature (K)

I_L - Light Generated Current (A)

I_o - Diode Saturation Current (A)

R_S, R_{SH} - Series and Shunt Resistance (Ω)

V - Cell Output Voltage (V)

With the provided equations and data mentioned, the maximum power of a given cell can be approximated.

2.5 The Performance Characteristics of Different PV Technologies

Several factors influence the performance of all photovoltaic modules, including solar irradiance level, operating temperature, soiling, solar spectrum, and the angle-of incidence at which sunlight strikes the module [10]. Other factors such as seasonal changes affect the performance of different modules and technologies as well. Studies are performed on existing and emerging technologies by collecting data over long periods of time and then analyzing its behavior. These studies have shown that amorphous silicon modules perform better and profit from improved efficiency as well as output power at higher operating temperatures during summertime and in warm climates, while it is the opposite for crystalline silicon modules [11][12]. Other studies also show that amorphous silicon arrays output between twenty and thirty percent more power than polycrystalline silicone arrays [14] in warmer climates. On the other hand, the performance of crystalline modules is based mostly on the amount of irradiation they are exposed to.

2.5.1 Energy Rating

Energy rating is based on the amount of energy a module produces over a certain amount of time under specific conditions [15]. Not all modules behave exactly the same, and even those that are rated at equal power capacity may not produce the same amount of energy over a given period of time. This is caused mostly to varying outputs when modules are deployed under different climatic conditions. For the end-user, an energy production approach is a better option than the power output rating at STC because it helps the user

compare the total average amount of energy produced over a period of time, versus just maximum power at certain conditions, that usually are not met simultaneously.

The National Renewable Energy Laboratory (NREL) has developed a consensus-based approach to rate PV modules based on the results of energy ratings by generating a Module Energy Rating (MER) process, and address the limitations of module power rating at Standard Test Conditions (STC) by proposing a method that consist of rating modules at five different reference days and two different load conditions [16][17]. Table 2-2 below represents the reference day's weather conditions. This method would ensure that modules are tested for energy production under several different climatic conditions instead of a set of one specific condition.

Table 2-2 Proposed Reference Days by MER Analysis

Profile	Irradiance (Peak W/m²)	Daytime High Temp (°C)	Wind Speed	Relative Humidity	Cloud Cover
Sunny-Hot	> 1000	> 35	Low	Low	0%
Sunny-Cold	> 900	< 0	Avg.	High	< 50%
Cloudy-Hot	< 400	> 30	Avg.	High	> 50%
Cloudy-Cold	200 to 400	< 0	High	High	> 90%
Average-Nice	800 to 900	20	Avg.	Avg.	30%

This method also suggests that a label such as a the one demonstrated in Figure 2-5, where X and Y are the measured values for watt-hour and amp-hour at the given reference day respectively, should be placed on the back of rated modules to let the user know the rated power at different conditions.

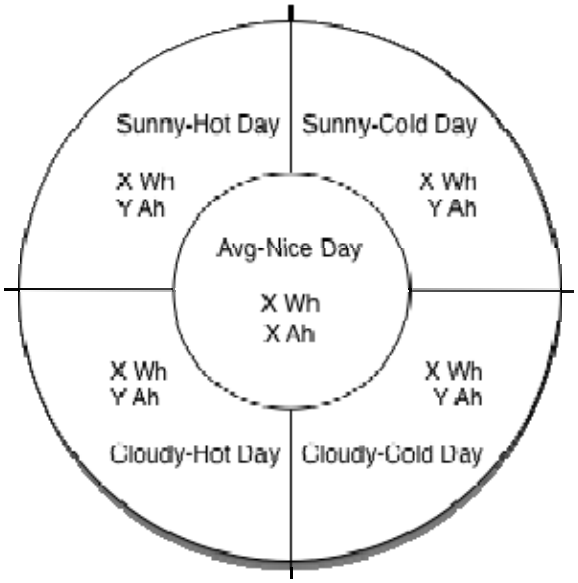

Figure 2-5 Proposed Rated Module Label

2.5.2 Performance Ratio (DC and AC)

PV technologies respond differently to the seasons of the year. Most performance ratios exhibit seasonal fluctuations largely correlated to air or module temperatures, varying between 80% and 100% and usually showing larger values during winter and lower performance during the summer, except for amorphous silicon and cadmium telluride modules [13]. These differences are mainly due to the varying temperature coefficients of the different technologies and their response to temperature differences.

The performance ratio analysis can be performed on either the AC or DC side of a PV system and allows for the performance analysis of different technologies for a given climate by normalizing global irradiation and without taking in consideration temperature at which the modules operate. Depending on the type of analysis interested, it can be performed in different time intervals, either on fifteen-minute intervals, hourly, daily,

monthly and yearly. Applying the performance ratio analysis on the DC side of a system allows to study the electrical performance of the system without taking into account any of the major losses found when converting the DC power produced by the array into AC power. On the other hand, applying the analysis on the AC side allows studying the total losses in the system. When both analyses are performed, inverter performance and system losses can be analyzed as well by applying Equation 2-4. Both analyses are important because they help study different aspects of the PV system.

$$\mu = \frac{PR_{AC}}{PR_{DC}} \qquad (2\text{-}5)$$

The final PV system yield Y_f is the net energy output E divided by the nameplate D.C. power P_0 of the installed PV array. It represents the number of hours that the PV array would need to operate at its rated power to provide the same energy. The Y_f normalizes the energy produced with respect to the system size; consequently, it is a convenient way to compare the energy produced by PV systems of different size [18][22]. Equation 2-6 represents the final yield of a PV array.

$$Y_f = \frac{E}{P_o} \qquad (2\text{-}6)$$

The reference yield Y_r is the total in-plane irradiance H divided by the PV's reference irradiance G. It represents an equivalent number of hours at the reference irradiance. It defines the solar radiation resource for the PV system and it is a function of the location, orientation of the PV array, and month-to-month and year-to-year weather variability [18][22]. Frequently the value G = 1,000 W/m^2 is used as reference because it represents

one of the parameters taken in consideration when performing tests at STC. Equation 2-7 represents the reference yield for a given PV array.

$$Y_r = \frac{H}{G} \qquad (2\text{-}7)$$

Finally, the performance ratio PR of a given PV system can be calculated by dividing the final yield by the reference yield. By normalizing with respect to irradiance, it quantifies the overall effect of losses ad the rated output due to: inverter inefficiency, wiring mismatch and other losses when converting from D.C. to A.C. power [18][22]. Equation 2-8 represents the performance ratio for a given system.

$$PR = \frac{Y_f}{Y_r} \qquad (2\text{-}8)$$

The overall performance of the system is also limited to the losses on the different components that allow the DC power generated to be converted to AC power. Table 2-3 below demonstrate different derate factor for AC power rating.

Table 2-3 Derate Factors for A.C. Power Rating [18]

Item	Typical	Range
PV Module Nameplate D.C. Rating	1.000	0.850 – 1.050
Initial Light-Induced Degradation	0.980	0.900 – 0.990
D.C. Cabling	0.980	0.970 – 0.990
Diodes and Connections	0.995	0.990 – 0.997
Mismatch	0.980	0.970 – 0.985
Inverter	0.960	0.930 – 0.960
Transformers	0.970	0.960 – 0.980
A.C. Wiring	0.990	0.980 – 0.993
Soiling	0.950	0.750 – 0.980
Shading	1.000	0.000 – 1.000
Sun-Tracking	1.000	0.980 – 1.000
Availability of System	0.980	0.000 – 0.995
Overall at STC	0.804	0.620 – 0.920

2.5.3 PVUSA (DC and AC)

The PVUSA (Photovoltaic for Utility Scale Applications) developed a rating methodology for PV performance evaluation, which has become popular, and even incorporated into concentrating PV rating standards. The method is based on collecting solar, meteorological, and system power output data for a period of time, and regressing the system power output, P, against a combination of irradiance, I, wind speed, W, and ambient temperature, T, variables in the form of equation 2-9 [19].

$$P = I(a + bI + cW + dT) \qquad (2\text{-}9)$$

The PVUSA method is based on the simplified assumptions that array current is primarily dependent on irradiance and that array voltage is primarily dependent on array temperature, which, in turn is dependent on irradiance, ambient temperature, and wind speed [23].

Once the regression is performed and the coefficients a, b, c, and d are calculated, values for PVUSA Test Conditions (PTC) are inserted in equation 2-9 and power, P, is calculated. The accepted values for PTC are usually the following:

- I = 1,000 W/m^2
- W = 1 m/s
- T = 20 °C

The relative contribution percent of each of the regression coefficients a, b, c and d are noted on Table 2-4 below.

Table 2-4 Relative Contribution for Each Regression Coefficient [19]

	a	b	c	d
Contribution	96.4 %	2.9 %	0.4 %	0.4 %

2.5.4 Inverter Performance Analysis

An inverter is a type of DC-to-AC converter that is installed along with a PV system to convert the DC energy produced from the solar array, or energy stored in batteries, into usable AC sinusoidal power. Several types of inverters exist for different applications and needs. The following three are the most popular.

a) Stand-Alone Inverters – Used when an electric grid is not connected to the PV system and usually has batteries attached to it to draw stored energy when production is not enough.
b) Grid-Connected Inverters – Works in parallel with an electric grid to convert the DC output from the array into consistent and synchronous AC power from the utility.
c) AC Module Inverter – Usually called micro-inverter, is a type of grid-connected inverter. These inverters are installed on every module of the array and replace the DC junction box.

The process of transforming DC power to AC power is not one hundred percent efficient; therefore some losses in the power conversion must be taken into account. Typical conversion efficiency is around ninety-three to ninety-six percent without considering other sources of losses such as DC and AC cabling and wiring [18]. Some input power is also used to operate the inverter electronics and keep the inverter in a powered

state at all times. Inverter efficiency is primarily affected by inverter load, but it can also be affected by inverter temperature and DC voltage input [4].

Figure 2-6 below represents a typical day of collected data at the Florida Solar Energy Center for a remote system. It is evident that the converted DC power from the array has a linear relationship with the AC power out of the inverter, and the conversion efficiency is around ninety-three percent.

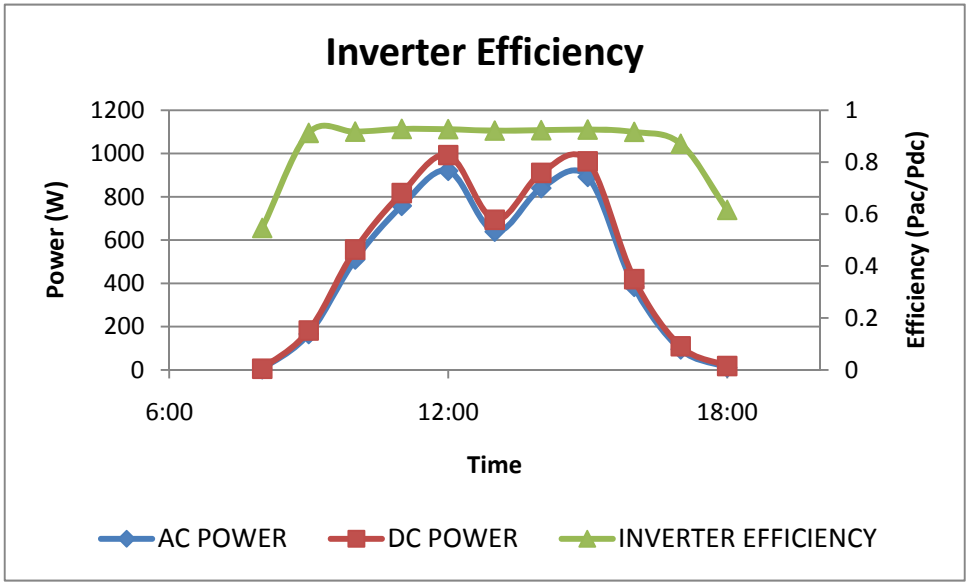

Figure 2-6 Inverter Efficiency

2.6 Summary of PV Analysis and Design Software

Three different software packages have been analyzed and are described in the subsections below. Some of these packages are more complex than others and some are available as freeware (SAM), while others are available as demos. Their features are briefly described.

2.6.1 Solar Advisor Model (SAM) 2010.4.12

The Solar Advisor Model (SAM) is a collaborative software project between the National Renewable Energy Laboratory (NREL) and Sandia National Laboratory that uses a system-drive approach (SDA) to establish the connection between market requirements and R&D efforts and how specific R&D improvements contribute to the overall system cost and performance [20].

The software combines a collection of PV module and inverter database with a collection of measured data for a typical meteorological year (TMY). The module and inverter database presents data provided in typical manufacturer specification sheets, such as P_{max}, V_{mp}, I_{mp}, V_{oc}, and I_{sc}, along with temperature coefficients, while the inverter database provides information such as inverter efficiency, minimum and maximum input voltage. On the other hand, the meteorological data provides hourly averages of data such as irradiation, total sky cover, and wind speed among others, at different locations throughout the United States.

By combining the abovementioned-collected data, the software allows the user to create a virtual system and predict monthly and year performance while considering a user specified degradation rate and allows for complex analysis of financial impact as well as shown in Figure 2-7 below.

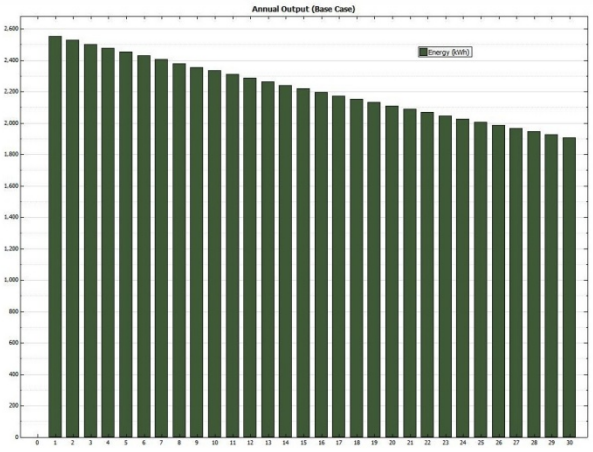

Figure 2-7 SAM 30 Year Energy Output and Degradation

2.6.2 Solar Pro 3.0

Solar Pro is a software program developed by Laplace Systems that allows researchers and engineers to simulate solar electric power systems. Similarly to SAM, it combines a series of databases that allow for such simulations to be performed. It contains solar irradiance and temperature data for over one thousand six hundred locations in the world, and provides module data for a variety of PV manufacturers. Contrary to SAM, Solar Pro allows the user to input a house or a building where the PV system will be installed, as well as input the surroundings, such as trees and other buildings, and simulate the energy output of the system based on the shading effect the surroundings will have. This tool helps designers find the optimum design in order to draw the most power out of the system. Figure 2-8 below shows the simulation of a PV array.

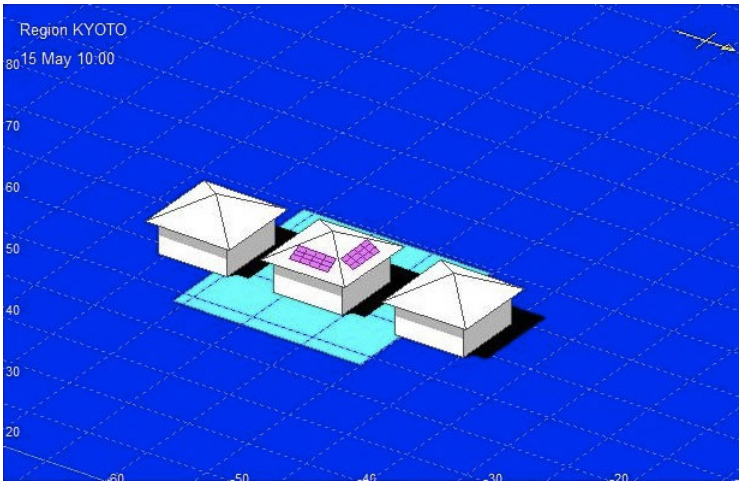

Figure 2-8 Solar Pro Shading Simulation

The software also allows the user to calculate the I-V curves of the different modules and their performance based on the specification sheets provided by the manufacturers. Similarly to SAM, Solar Pro also provides the user with a comprehensive financial analysis that allows the user to understand the impact of installing such system. Figure 2-9 shows a comprehensive analysis of the average energy production, PV temperature, air temperature, PV voltage and irradiation for a full year.

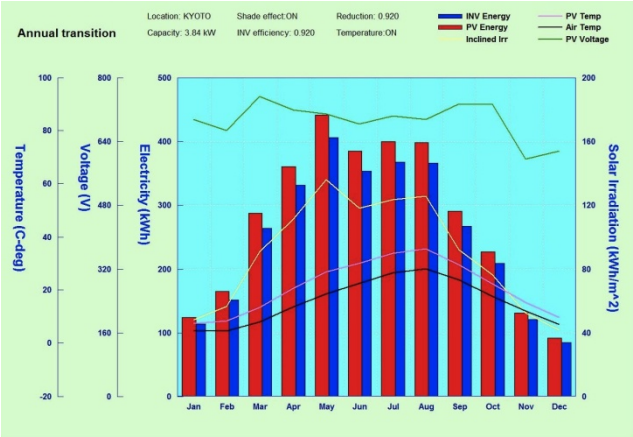

Figure 2-9 Solar Pro 3.0 Summary of Average Data

2.6.3 PVSyst 5.12

PVsyst is a software package that similarly to SAM and Solar Pro, that combines the engineering aspects with the financial portion of installing and managing a PV system. It contains a database of over one thousand seven hundred and fifty PV modules, and over six hundred and fifty inverters, and like Solar Pro, lets the user design a building and its surroundings to determine energy production based on shading effects. It does this by combining the meteorological data with the specifications of the system, including system capacity, installation angle, location, and orientation. Contrary from SAM and Solar Pro, PVsyst allows the user to input information about the loads and the daily consumption, allowing for better accuracy of the design phase. Figure 2-10 shows a one-year average of data calculated by PVsyst.

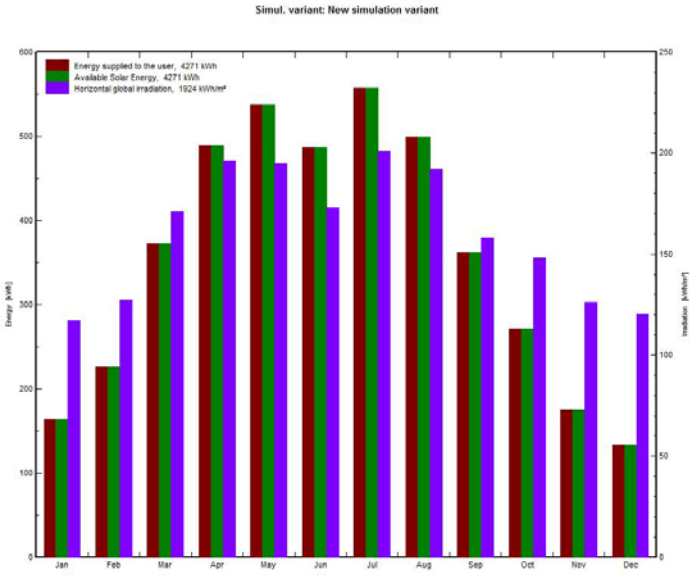

Figure 2-10 PVSyst 5.12 Sample Output Data

CHAPTER 3 PV MODULE AND SYSTEM TESTING, MONITORING AND ANALYSIS AT FSEC

3.1 FSEC PV Characterization Facilities and Module Testing

FSEC has been highly involved in testing both commercially available PV modules as well as prototypes not yet ready for industry. The testing here consists of indoor module tests performed with a solar flash simulator, which allows for highly repeatable experiments, as well as outdoor testing performed with highly sensitive measurement instrumentation.

Testing and characterization of current PV technologies is important in order to ensure the continuous development of future technologies. Using decades of experience in photovoltaic research development, design, testing and applications, FSEC reviews each PV system design for compliance with the National Electrical Code (NEC) and the appropriate use of accepted design practices [24]. Not only module testing and research is performed at the Florida Solar Energy Center. FSEC has also partnered with Sandia National Laboratories (SNL), the Southwest Technical Development Institute (SWTDI), and the California Energy Commissions Public Interest Energy Research (CECPIER) to characterize the performance of PV inverters operating over extended periods of time [25]. Figure 3-1 exhibits FSEC's outdoor testing facility.

Figure 3-1 FSEC Outdoor Testing Facility

3.1.1 Outdoor Module Testing and Characterization

Current-Voltage (I-V) characteristics are often measured during outdoor module testing using an I-V curve tracer, and they describe the relationship of current with respect to voltage. These curve tracers measure the POA irradiance and the module temperature as well and are often used to measure temperature coefficients of modules. Figure 3-2 below demonstrates an example of three I-V curves measured on a p-Si module.

The following is a list of different kind of module testing that can be performed at FSEC's outdoor testing facility:

a) Fixed Rack Testing – Done in order to calculate outdoor performance of PV modules with module aging.
b) Temperature Coefficients Test – This type of testing is done to calculate the values for current, voltage, and power temperature coefficients. It can also be performed indoors with a solar simulator where the testing atmosphere can be controlled.

c) Irradiance Test – Performed to measure internal resistance of the PV modules. This data is compared with indoor measured data using the solar simulator.

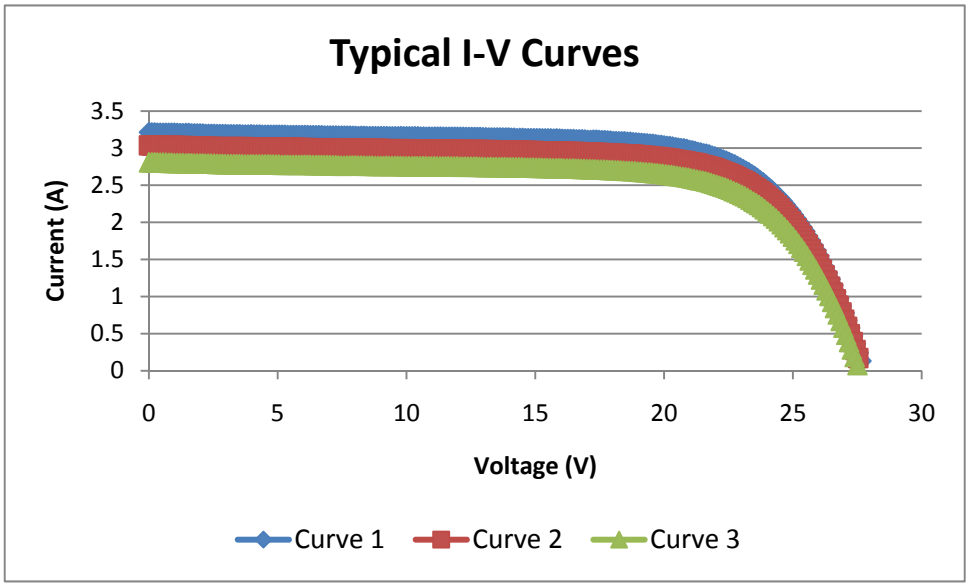

Figure 3-2 Sample I-V Curves Measured on a p-Si module

3.1.2 Indoor Module Testing and Characterization

FSEC's module testing laboratory is equipped with a SPI-SUN 660 flash simulator that is used as part of the PV module certification process and has also upgraded its laboratory facilities and instituted an ISO/IEC 17025:2005 quality system [24]. The following kinds of testing can be performed in the indoor testing facilities:

a) STC Power Rating – The objective of this kind of test is to determine how the electrical performance of the modules varies with load at STC. Test instrumentation should be as stipulated on IEC standards for either crystalline or thin-film modules.

b) Temperature Coefficients Test – The objective is to gather data to calculate temperature coefficients using the solar simulator. This test can usually be

performed in less than one day, saving time when multiple modules have to be tested.

c) Irradiance Test – This test is done to calculate the internal resistances of PV modules and compare it with outdoor test data.

IEC testing standards for indoor testing must be followed at all times. I-V curve readings must be within a ±0.2% at all times, and module temperature within ±1 °C.

3.2 FSEC PV System Field Testing and Monitoring

For years, FSEC has monitored the performance of many PV systems installed through the state of Florida and beyond. The data collection system consists of automated on-line data collection, storage, management and analysis of real-time and historical data, and custom presentation interfaces. The data is collected from private homes, schools or universities and then retrieved to perform different studies, such as de degradation analysis performed in this thesis. Table 3-1 below demonstrates all systems for which FSEC has collected data.

Table 3-1 FSEC Monitored Systems

PV System Name	Location	Size Watts	Install Date	DAS
A Child's Place	Jacksonville	6160	10-SEP-03	ACP
A. D. Henderson University	Boca Raton	5000	20-OCT-03	HEN
Adams Home	Lakeland	4050	01-MAR-98	PVR
Admiral Farragut Academy	St. Petersburg	2100	01-JUL-07	AFA
Anderson School for the Arts	Jacksonville	3960	28-SEP-00	
Ardila Home	New Smyrna B	3600	14-DEC-01	
Baldwin High School	Baldwin	3960	01-SEP-00	
Bartos Home	New Smyrna B	2400	03-DEC-01	
Bay High School	Panama City	3960	19-MAR-04	BAY
Bidgood Home	New Smyrna B	2400	15-MAY-00	
Boone High School	Orlando	3600	19-DEC-01	
Celebration School	Celebration	3960	08-DEC-03	CEL
Center for Advanced Power Systems	Tallahassee	5940	15-DEC-03	FSU

Central Florida Electrical JATC	Winter Park	3600	01-DEC-03	CFJ
Colonial High School	Orlando	3600	20-AUG-01	
Coronado Beach Elementary School	New Smyrna B	4050	01-JUN-99	COR
Crystal Lake Middle School - PC2	Lakeland	1800	01-JUL-99	
Crystal Lake Middle School - PC3	Lakeland	1800	01-JUL-99	
Daytona Beach JATC	Daytona Beach	4000	28-JUN-04	DBJ
Dion Home	New Smyrna B	2400	12-MAR-01	
Disney Wilderness Preserve- The Nature C	Kissimmee	4140	01-SEP-99	DW1
Disney Wilderness Preserve- The Nature C	Kissimmee	2340	01-SEP-99	DW2
Dr. Phillips High School	Orlando	3600	24-AUG-01	
Dunlop Home	Cocoa	2240		
Edgewater High School	Orlando	3900	01-OCT-00	OUC
Edgewood Jr-Sr High School	Merritt Isla	2050	08-APR-08	EHS
Energy Conservation Services	Gainesville	1200	15-DEC-02	
Englewood High School	Jacksonville	3960	28-SEP-00	
Epsicopal High School	Jacksonville	4760	02-SEP-03	EPS
Evens Home	Weirsdale	1280	15-FEB-02	MF6
FAMU/FSU College of Engineering	Tallahassee	5940	15-DEC-03	FAM
FCCJ	Jacksonville	2040	02-AUG-02	
First Coast High School	Jacksonville	4200	26-MAY-00	
Florida Community College	Jacksonville	3960	21-SEP-00	
Florida Gulf Coast University	Fort Myers	4760	08-OCT-03	FGC
Florida Solar Energy Center	Cocoa	9720	01-DEC-08	SOL
Florida Tech	Melbourne	4800	20-DEC-03	FIT
Forest High School	Ocala	2100	30-JAN-07	FST
Forrest High School	Jacksonville	3960	20-SEP-00	
G. W. Robinson Builders	Gainesville	1800	15-DEC-02	
Gainesville Electrical JATC	Gainesville	4800	30-JAN-04	GAJ
Gainesville Regional Utilities	Gainesville	10000	01-JUN-95	
George Jenkins High School - P11/PC10	Lakeland	1800	01-JUL-99	
George Jenkins High School - P15/PC8	Lakeland	1800	01-JUL-99	
George Jenkins High School - P17/PC12	Lakeland	1800	01-JUL-99	
George Jenkins High School - P4/PC17	Lakeland	1800	01-JUL-99	
George Jenkins High School - P8/PC2	Lakeland	1800	01-JUL-99	
Gillen Home	Haines City	960	22-NOV-01	MF5
Hammerstrom Home	Key Largo	2880	01-JUN-02	JHK
Hard Bargain Farm	Accokeek	12000	18-NOV-04	HBF
Harllee Middle School	Bradenton	4760	09-OCT-03	HAR
Helfrich Home	Orlando	2400	27-JUN-02	
Homosassa Elementary School	Homosassa	2000	01-MAY-07	HES
JEA Plaza III	Jacksonville	4906		
JEA Plaza III	Jacksonville	2580		
JEA Plaza III	Jacksonville	2580		
Jackson High School	Jacksonville	3960	24-AUG-00	
Jacksonville JATC	Jacksonville	12000	07-JUL-03	JET
Junior Museum	Panama City	3960	01-JAN-01	JRM
Kanapaha Middle School	Gainesville	1680	15-JAN-04	KMS

Kessinger Home	New Smyrna B	2400	01-MAR-02	
Krallinger Home	Debary	960	28-JAN-02	MF3
Lake Gibson High School - P11/PC2	Lakeland	1800	01-JUL-99	LP4
Lake Gibson High School - P14/PC6	Lakeland	1800	01-JUL-99	LP3
Lake Gibson High School - P5/PC15	Lakeland	1800	01-JUL-99	
Lake Gibson Middle School - PC2	Lakeland	1800	01-JUL-99	
Lake Gibson Middle School - PC4	Lakeland	1800	01-JUL-99	
Lake Gibson Middle School - PC6	Lakeland	1800	01-JUL-99	
Lake Sybilia Elementary School	Maitland	2004	19-JAN-07	LSS
Lakewood High School	St. Petersbu	3960	12-NOV-03	LWD
Lary Home	Homestead	4800	29-APR-02	TLH
Lee High School	Jacksonville	3960	01-SEP-00	
Leird Home	Lakeland	2025	01-APR-98	LP1
Lerner Home	Bonita Sprin	2048	31-MAY-02	
Loggerhead Key	Dry Tortugas	14400	01-MAY-02	LHK
Lyman High School	Longwood	3960	02-DEC-03	LYM
Lynn Home	Rockledge	2400	20-JUL-02	KEV
MAST Academy	Miami	2000	29-JUN-07	MAS
Manatee Technical Institute	Bradenton	1980	01-APR-08	MTI
Mandarin High School - East	Jacksonville	3960	29-SEP-00	
Mandarin High School - West	Jacksonville	3960	29-SEP-00	
Martin Power Plant	Indiantown	9975	01-AUG-99	
McKerley Home	Pensacola	2880	10-DEC-02	
McLaughlin Home	Winter Garde	800	26-FEB-02	MF2
Meigs Middle School	Shalimar	3960	05-FEB-03	MMS
Melone Home	Delray Beach	2400	17-JUN-02	
Middleton High School	Tampa	10500	27-MAR-07	MHS
Murphy Home	Apollo Beach		01-AUG-00	
Museum of Science and Industry	Tampa	14000	02-MAR-00	
NSB Municipal Golf Course	New Smyrna B	4800	19-MAR-02	
Nature Coast Technical High School	Brooksville	3960	15-JAN-04	NCT
New Smyrna Beach Middle School	New Smyrna B	600	28-JUN-04	NMS
OSullivan Home	New Smyrna B	2400	29-OCT-01	
Ocoee Elementary School	Ocoee	3600	02-JUN-03	OCE
Ocoee Middle School	Ocoee	3600	05-DEC-03	OCM
Olympia High School	Orlando	2004	09-DEC-08	OHS
Palazzotto Home	New Smyrna B	3360	01-FEB-00	ZE2
Palm City Elementary School	Palm City	2000	29-JUN-07	PCE
Parish Home	Tarpon Springs	2160	04-JAN-02	
Parker High School	Jacksonville	4080	16-NOV-99	
Parker High School - East	Jacksonville	3960	29-SEP-00	
Patelunas Home	Haines City	960	25-JAN-02	MF4
Paxon School for Advanced Studies	Jacksonville	3960	28-SEP-00	
Pelotes Island	Jacksonville	4000	01-JUN-83	
Peters Home	New Smyrna B	1200	08-SEP-00	
Peterson Academies of Tech.	Jacksonville	3960	20-SEP-00	
Polk Ave. Elementary School	Lake Wales	2100	01-MAY-07	PAE

Progress Energy	Orlando	15000	23-AUG-88	
Publix #1129	Miami Lakes	26112	01-AUG-08	
Publix #1157	Palm Beach G	26112	25-NOV-08	
Publix #1159	Boca Raton	26112	01-JUN-08	
Publix HQ	Lakeland	24000	01-NOV-08	
Raines High School	Jacksonville	4080	05-MAY-00	
Randolph Academies of Tech.	Jacksonville	3960	24-AUG-00	
Ribault High School	Jacksonville	3960	21-SEP-00	
Ridenour Water Treatment Station	Jacksonville	4560	07-JUL-00	
Robinswood Middle School	Orlando	3600	20-SEP-01	
Rollins College	Winter Park	1600	01-MAY-07	
Romero Home	Winter Garden	1200	10-AUG-01	MF1
Rothenbach Park	Sarasota	250000	01-OCT-07	
Sikes Elementary School - PC10	Lakeland	1800	01-JUN-00	
Sikes Elementary School - PC11	Lakeland	1800	01-JUN-00	
Smith Home	Jacksonville	1800	20-DEC-02	
Solar Energy Inc.	Jacksonville	6000	20-DEC-02	
Solar Source	Largo	1200	04-DEC-02	
South Miami High School	Miami	2000	29-JUN-07	SMH
Southface Energy Institute	Atlanta	1666	01-JAN-02	SFI
St. Pete High School	St. Petersburg	4008	29-NOV-07	SPH
St. Thomas University	Miami	2400	01-AUG-02	STU
Stanton College Prep. School - East	Jacksonville	3960	28-SEP-00	
Stanton College Prep. School - West	Jacksonville	3960	28-SEP-00	
Stein Home	Gainesville	1800	05-FEB-02	
Stonerock Home	Orlando	5400	01-APR-02	
Sullivan Home	Ocala	1800	21-DEC-01	
Szaro Home	Merritt Isla	1200	20-JUL-02	JEN
Tallahassee City Utilities	Tallahassee	9962	25-APR-00	TAL
Tallahassee City Utilities	Tallahassee	18000	01-JUN-94	
Tampa Electric JATC	Tampa	2100	15-NOV-07	TAJ
The Bolles School	Jacksonville	4760	02-SEP-03	BOL
Traviss Technical Center - PC3	Lakeland	1800	01-JUL-99	
Traviss Technical Center - PC6	Lakeland	1800	01-JUL-99	
Tuskawilla Montessori Academy	Oviedo	2100		TMA
Varnedoe Home	Tallahassee	3840	23-JAN-02	
Warner Solar	Navarre	2400	04-JUL-02	
Warren Home	Lakeland	1800	04-JAN-98	LP2
Waterford Elementary School	Orlando	2100	01-DEC-07	WES
West Florida High School	Pensacola	3960	05-SEP-03	WFH
Westside Tech	Winter Garden	9600	31-JUL-02	
Westside Tech	Winter Garden	3600	02-JUN-03	WST
Westwood Middle School	Gainesville	1680	15-JAN-04	WMS
White High School	Jacksonville	3960	20-SEP-00	
Willett Home	Ft. Pierce	2400	04-JUN-02	
Wolfson High School	Jacksonville	3960	25-SEP-00	
Zarillo Home	Melbourne	1800	01-DEC-02	

Once the data is stored, it can be either be downloaded or the server will automatically generate day-by-day analysis of the collected data. Figure 3-3 below represent two plots generated by the system that demonstrate exactly this.

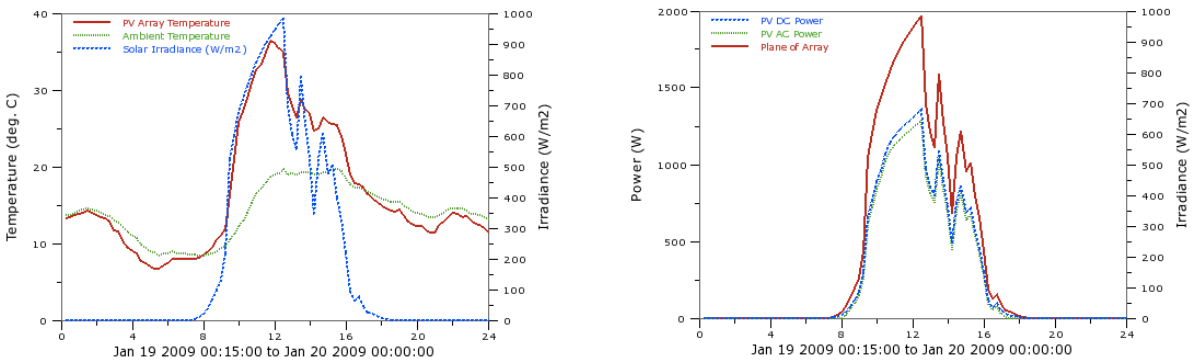

Figure 3-3 Last day of Data for KMS System (PV Temperature & Solar Irradiance)

3.2.1 Overview of the PV System Test Instrumentation

In order to collect and monitor data, different models of Campbell Scientific data loggers, such as CR10, CR10X, and CR1000, along with other sensors were installed on the different PV sites. The data monitored shown in Table 3-2 is stored on a server at FSEC and can be accessed using any web browser. It can later be downloaded and imported into spreadsheet software for manipulation and analysis.

Table 3-2 Parameters Measured and Instrumentation

Parameter	Instrumentation
DC Current (A)	Empro Current Shunt-
DC Voltage (V)	Voltage Divider
AC Power (W)	IMS Meter w/ Pulse Output
POA Irradiance (W/m^2)	Li-Cor LI200 Pyranometer
Module Temperature (°C)	Type T Thermocouple Wire
Ambient Temperature (°C)	Type T Thermocouple Wire

3.2.2 Monitored Parameters

PV modules behave differently, according to the meteorological conditions in which they operate. On one hand, voltage behaves as a function of the temperature of the module, and on the other, current behaves as a function of the incident irradiance on the module. Therefore, it is imperative that DC current, DC voltage and AC Power data be recorded as well as the POA irradiance and ambient and module temperature.

3.2.2.1 Meteorological

Meteorological measurements consisted of data recorded for the ambient temperature and irradiance. Pyranometers, which devices that measure solar radiation flux density, were installed at the same tilt angle and orientation of the array to ensure incident irradiation data was collected. Pyranometers are usually calibrated outdoors under clear sky conditions by using a calibrated reference pyranometer. It is important to have well calibrated pyranometers installed when measuring and monitoring data in order to obtain reliable and trustworthy data sets that can be studied. Figure 3-4 below demonstrates an installed pyranometer.

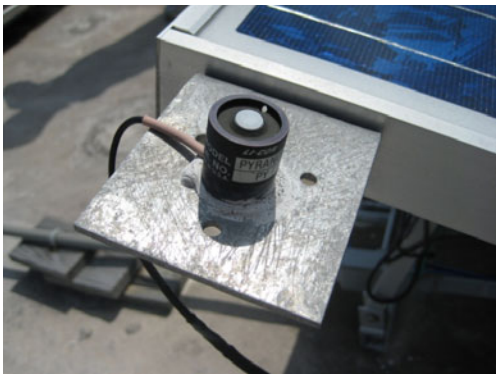

Figure 3-4 Installed Pyranometer

3.2.2.2 PV Output

PV output measurements consist of DC current and voltage produced by the array, and AC Power converted by the inverter. PV output current and voltage depend primarily of total POA irradiance and module temperature, respectively. The effect of how module output current is affected by incident POA irradiance is demonstrated in Figure 3-5 below.

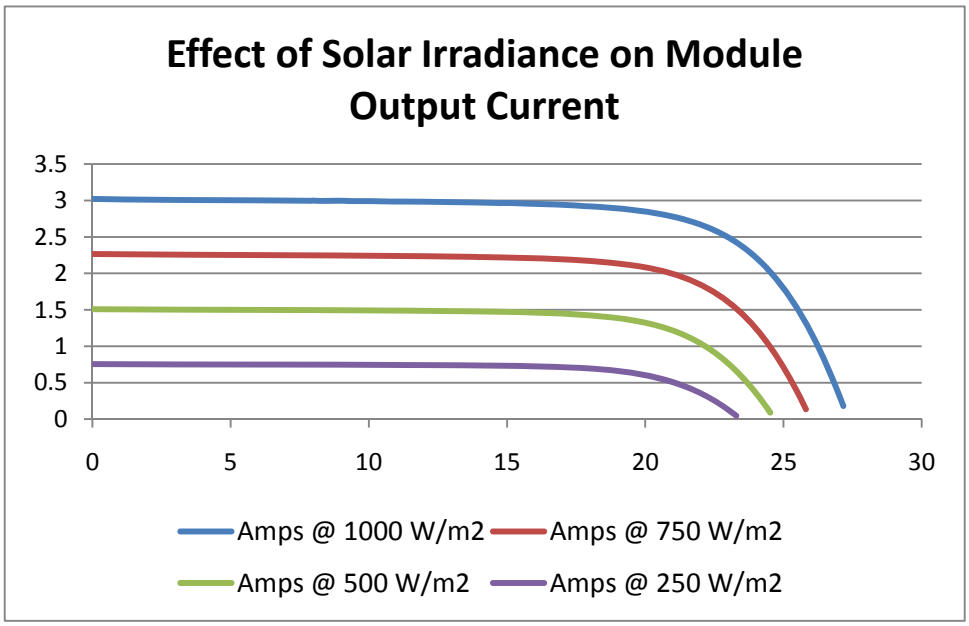

Figure 3-5 Effects of Solar Irradiance on Module Output Current

On the other hand, the effect of module temperature on PV module output is demonstrated on Figure 3-7.

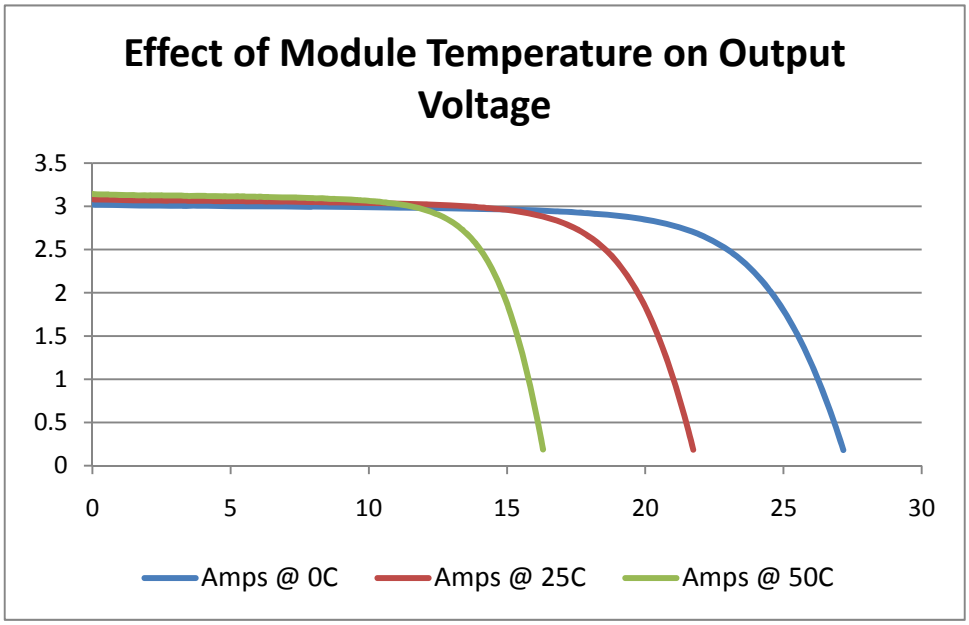

Figure 3-6 Effect of Module Temperature on Output Voltage

Because DC current and voltage is measured using the instruments mentioned in Table 3-2, DC power doesn't have to be measured, but it can be calculated by applying Equation 3-1.

$$P_{DC} = I_{DC}V_{DC} \qquad (3\text{-}1)$$

3.2.2.3 Module Temperature

Module temperature is measured by placing a thermocouple on the back of the module. A thermocouple is a device that produces a voltage from a junction of two metals that is related to a temperature difference. There exist several types of thermocouples for a variety of applications and they are usually inexpensive. Figure 3-7 below demonstrates a sample thermocouple installed in the back of a module.

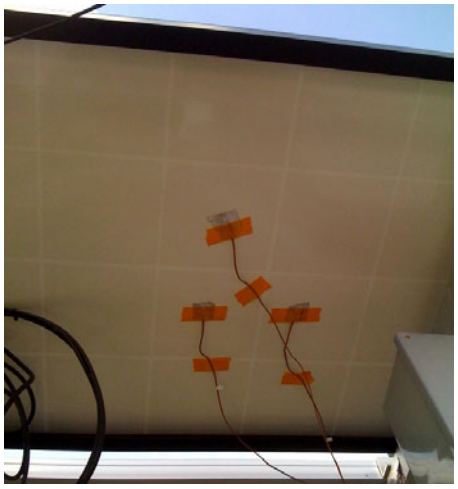

Figure 3-7 Installed Thermocouples

3.2.2.4 Data Acquisition Systems and Monitoring Systems Operationg

A data logger is a device that collects and records data for a period of time. The data can later be retrieved by the end-user to analyze it. The different channels of the data loggers installed at the various PV sites studied here were sampled every second and fifteen-minute averages where calculated for every value being recorded. Figure 3-8 below shows a DAS installed at the MMS system.

Figure 3-8 DAS at MMS System

CHAPTER 4 EVALUATION OF PV PERFORMANCE

4.1 Data Set Construction

Since the 1990's the Florida Solar Energy Center has been collecting data from different PV sites in the state of Florida, including schools, houses and universities, among others. For years, these sites have been contributing with valuable data that today can be used to study degradation rates, performance, and service lifetime of different field-aged PV technologies.

As the PV systems are installed, sensors and transducers that measure data every second, such as irradiance, voltage, current, power and temperature are also installed. Measured data is collected by the data logger and sent over an Internet connection to FSEC's servers. This data collected is then averaged to create fifteen-minute averages data points that are later used for different type of analyses. Figure 4-1 below presents a flow chart of the data collection process.

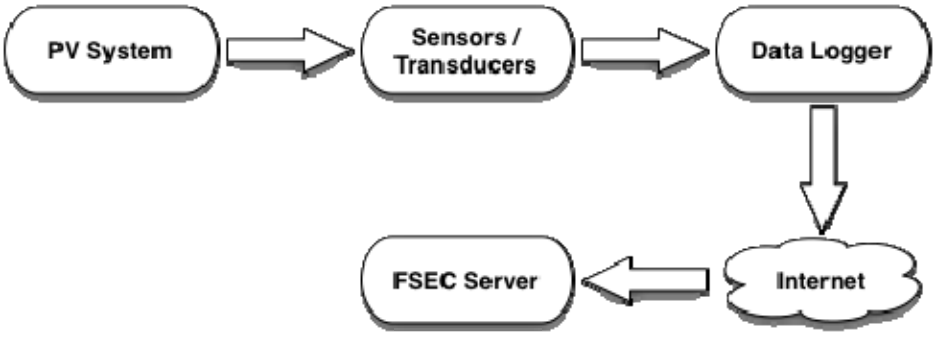

Figure 4-1 Data Set Construction Flow Diagram

Five systems in the state of Florida have been selected to perform the degradation studies presented. Figure 4-2 below shows a map with the location of the systems selected for the analysis while Table 4-1 shows general system information for each of the five selected systems.

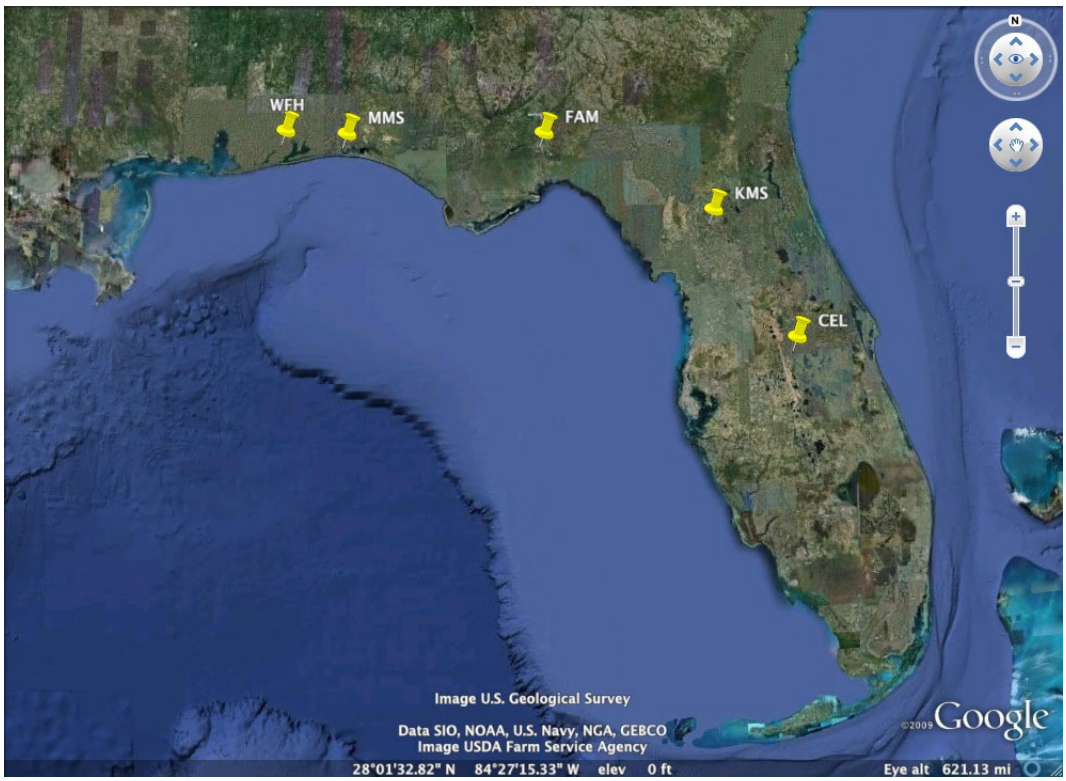

Figure 4-2 Map of Selected Systems

Table 4-1 General System Information

System	Size (W)	Technology	Install Date	Years	Azimuth & Tilt
CEL	3960	p-Si	12/8/03	3	225° West of South; 15°
FAM	5940	p-Si	12/15/03	5	208° West of South; 25°
KMS	1980	m-Si	1/15/04	4	180° South; 17°
MMS	3960	p-Si	2/5/03	4.5	180° South; 25°
WFH	3960	p-Si	9/5/03	2.5	180° South; 22.5°

4.2 Monthly Meteorological Data

The energy produced by a grid connected photovoltaic system depends on climatic factors, mainly the incident radiation on the modules and the temperature of work of such, which is function mainly of the radiation and the ambient temperature [29]. For every system monitored and that FSEC has collected data, this important meteorological information has also been recorded and will later be used to analyze the performance and the degradation of the systems studied. The data logger is constantly collecting data, and it is later separated as shown is Table 4-2 below.

Table 4-2 Monthly Meteorological Data (*in case of leap years)

Month	Days	Month	Days
January	1 - 31	July	182 - 213
February	32 - 59	August	214 - 244
March	60 - 90	September	245 - 274
April	91 - 120	October	275 - 305
May	121 - 151	November	306 - 334
June	152 - 181	December	335 - 365/366*

4.3 Module Input Data Sets and Restrictions

The process for data selection and validation is not a complicated one. After the collected data from the different FSEC monitored PV sites is retrieved, the filtering process begins. As mentioned before, not all the data acquired is valid since network failures can cause data not to be stored properly, therefore this kind of data is filtered out. The following are three sets of restrictions used to obtain two data sets from each PV system:

- Daylight only data – eliminates times of day where irradiance is too low to produce enough power and makes sure any type of shadow does not cover the

array, assuming that low irradiation measurements could mean shaded array and not only shaded pyranometer.

  - 500 – 1200 W/m^2
  - 800 – 1200 W/m^2

- Ambient Temperature – eliminates data points where the temperature is too low or too high, usually erroneous data, that do not fit the profile of the region being studied.
  - -20 – 60 °C
- Not shaded array – eliminates data points where more than 25% of the array is shaded.

Figure 4-3 below shows raw data for three of the five systems that were used for this study.

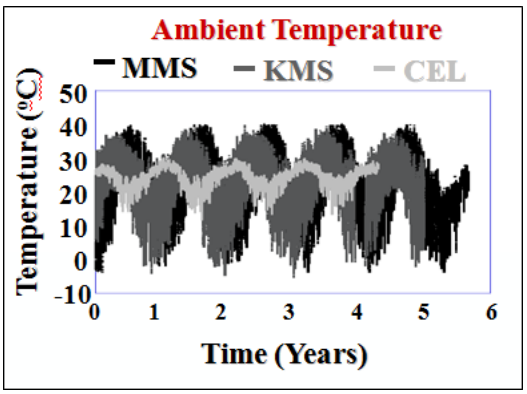

Raw Data (Amb. Temperature)

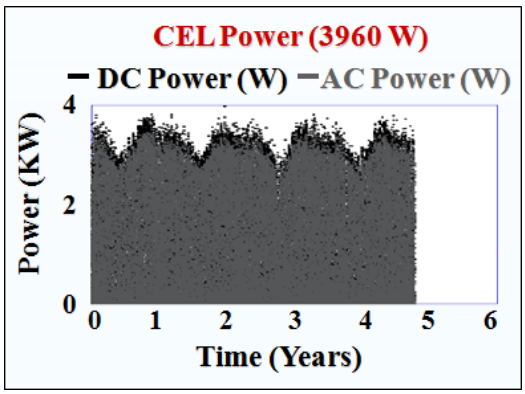

CEL Raw Data (Power)

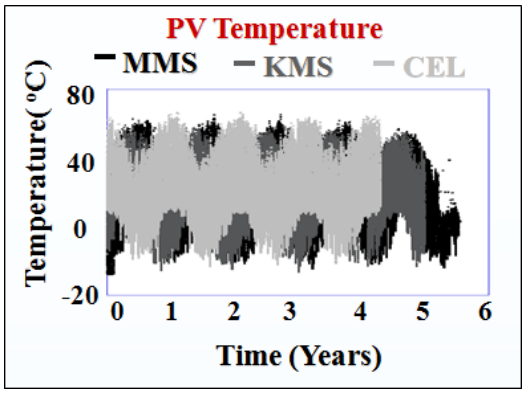

Raw Data (PV Temperature)

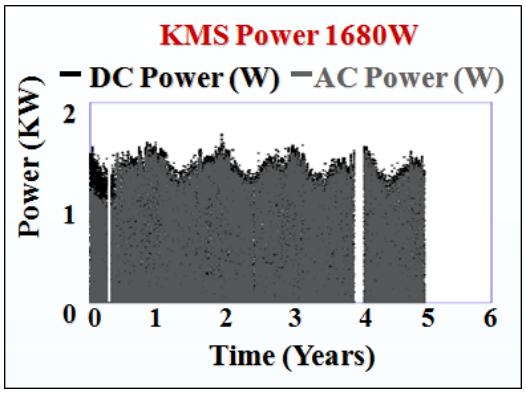

KMS Raw Data (Power)

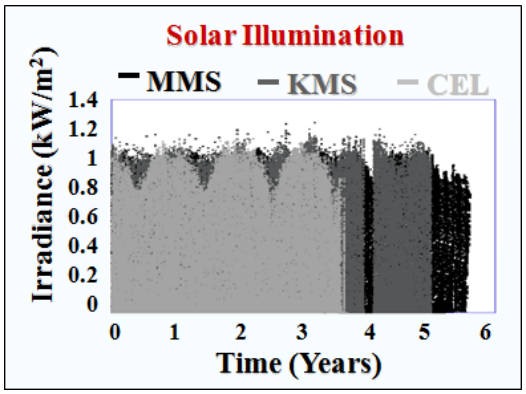

Raw Data (Solar Illumination)

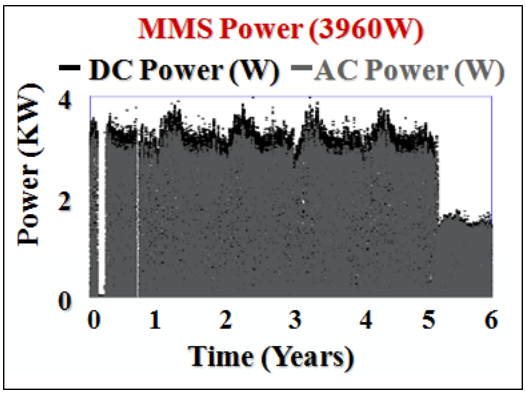

MMS Raw Data (Power)

Figure 4-3 Raw Data

When filtering the data only valid data is kept, making the analysis easier and eliminating errors. Of course, some problems are present when filtering the data too much, especially when filtering irradiance in the 800-1200 W/m^2 in months like November, December and January. Because of the orientation of the Earth and the region being studied, it is sometimes hard to get irradiance as high as 900 W/m^2, therefore only these restrictions where used to filter the data and the remaining data consisting of module

temperature and AC and DC power is kept, as these are the parameters to be used in the analysis.

Once the data sets are filtered, two sets are obtained for different irradiance ranges and a constant range for ambient temperature, followed by two distinctive analysis methods.

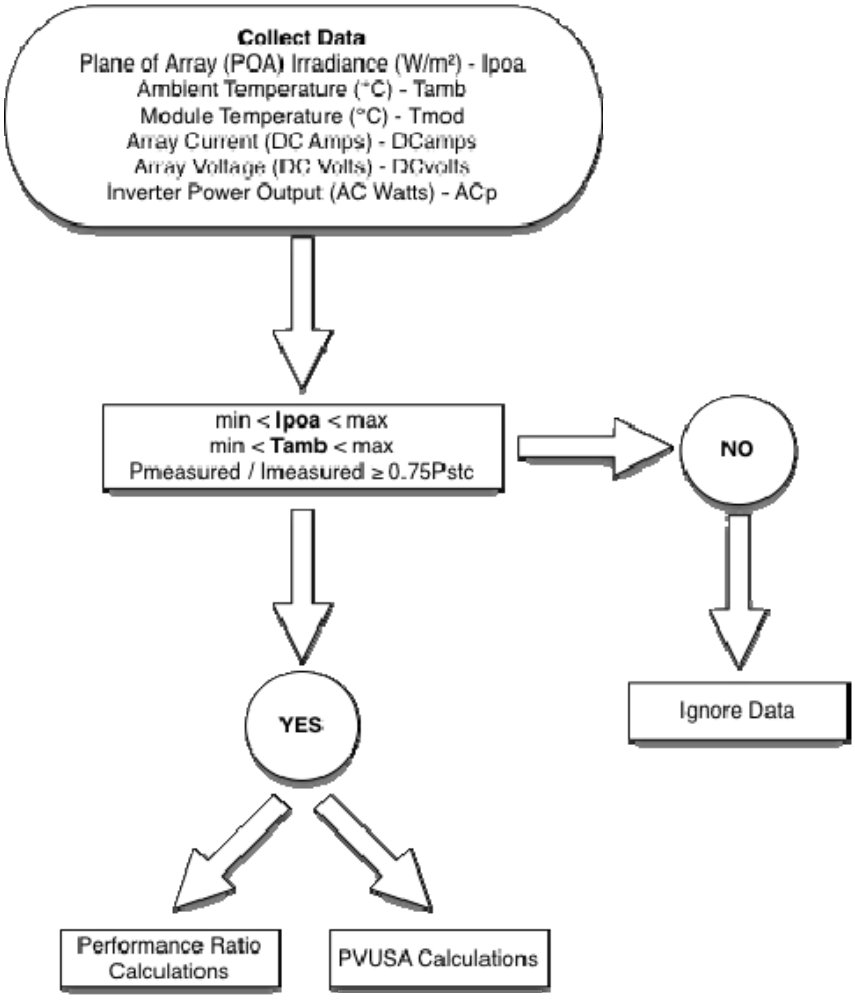

Figure 4-4 Data Selection Flow Diagram

4.4 Data Analysis Methods

Throughout the years, researchers and developers alongside with industry and manufacturers have come up with different type of analyses to better qualify and quantify degradations rates and estimate service time of field aged PV modules. Two widely accepted analyses, the Performance Ratio analysis the PVUSA Regression, are to be examined and compared in order to find acceptable degradation rates for different PV modules installed.

As mentioned in section 4.3, Module Input Data Sets and Restrictions, the total amount of incident irradiance has been filtered in two ranges, with the purpose of examining the degradation of the systems at these two windows of irradiance. Table 4-3 and 4-4 below show the results obtained by performing each of these analyses on the collected data. Such results are obtained by means of a MATLAB subroutine (Appendix A) that takes a Microsoft Excel file as an input, prompts the user for some system data and location of parameters in the Excel sheet, and then cycles through all the data (divided by months) performing the analysis and outputting an Excel file with the analyzed data, including the PVUSA power for both AC and DC, and the performance ratio for both AC and DC as well. The PVUSA analysis performed in this study does not take into account the speed of wind, which as stated in Equation 2-9, corresponds to the value of 'c'. This value contributes to only 0.4% of the total PVUSA power calculated [19].

Table 4-3 Calculated Degradation Using Performance Ratio (%/year)

System	PR AC (500-1200 W/m²)	PR DC (500 – 1200 W/m²)	PR AC (800 – 1200 W/m²)	PR DC (800 – 1200 W/m²)
CEL	-2.69 %	-2.73 %	-2.42 %	-2.49 %
FAM	-0.68 %	-0.51 %	-0.76 %	-0.57 %
KMS	-1.46 %	-1.44 %	-1.57 %	-1.60 %
MMS	-0.40 %	-0.33 %	-0.38 %	-0.31 %
WFH	-1.08 %	-1.07 %	-1.03 %	-1.02 %

Table 4-4 Calculated Degradation Using PVUSA Regression (%/year)

System	PVUSA AC (500 – 1200 W/m²)	PVUSA DC (500 – 1200 W/m²)	PVUSA AC (800 – 1200 W/m²)	PVUSA DC (800 – 1200 W/m²)
CEL	-2.31 %	-2.34 %	-2.29 %	-2.39 %
FAM	-0.69 %	-0.48 %	-0.62 %	-0.39 %
KMS	-1.93 %	-1.96 %	-2.16 %	-2.18 %
MMS	-0.82 %	-0.75 %	-1.10 %	-1.01 %
WFH	-4.34 %	-4.40 %	-2.31 %	-2.30 %

4.5 Annual PV Performance Prediction

As previously mentioned, monthly performance has been calculated for five different systems using the PVUSA Regression and the Performance Rating analysis. The energy output for each system can also be modeled and estimated over a period of time using a straightforward technique utilizing the nameplate power output of the array along with the Performance Rating values and the degradation rates established from the experimental results [30]. Equation 4-1 below is used to estimate the energy output for a period of twenty years.

$$E = H * N * P_{STC} * PR \qquad (4\text{-}1)$$

where,

H - Average Irradiation per Day (kWh/m^2/day)

N - Number of Days in the Month (day)

P_{stc} - Nameplate Power at STC (kW/kW/m^2)

PR - Experimentally Calculated Performance Ratio (unit less)

E - Calculated Energy Output, for either AC or DC sides (kWh)

Figures 4-5 to 4-9 represent an estimated energy output per month for twenty years using the above-mentioned technique. NREL's Red Book was used to find the average irradiation per day as shown in Table 4-5 below.

Table 4-5 NREL Red Book Average Irradiation Per Day

Month	**Jan**	**Feb**	**Mar**	**Apr**	**May**	**June**	**Jul**	**Aug**	**Sep**	**Oct**	**Nov**	**Dec**
Ave. kW/m^2/day	4.3	4.9	5.7	6.3	6.0	5.5	5.5	5.6	5.3	5.0	4.6	4.1

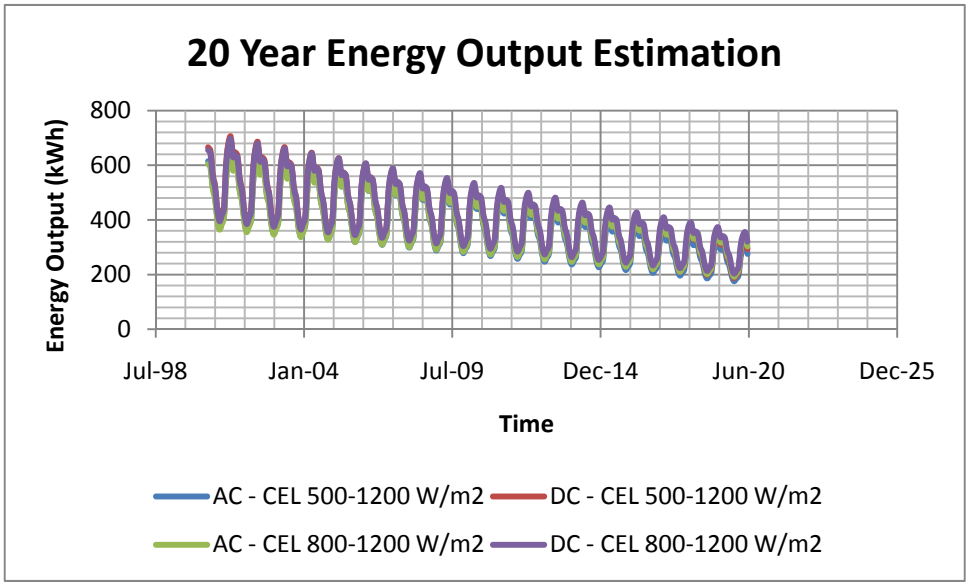

Figure 4-5 CEL Energy Output Prediction for 20 Years

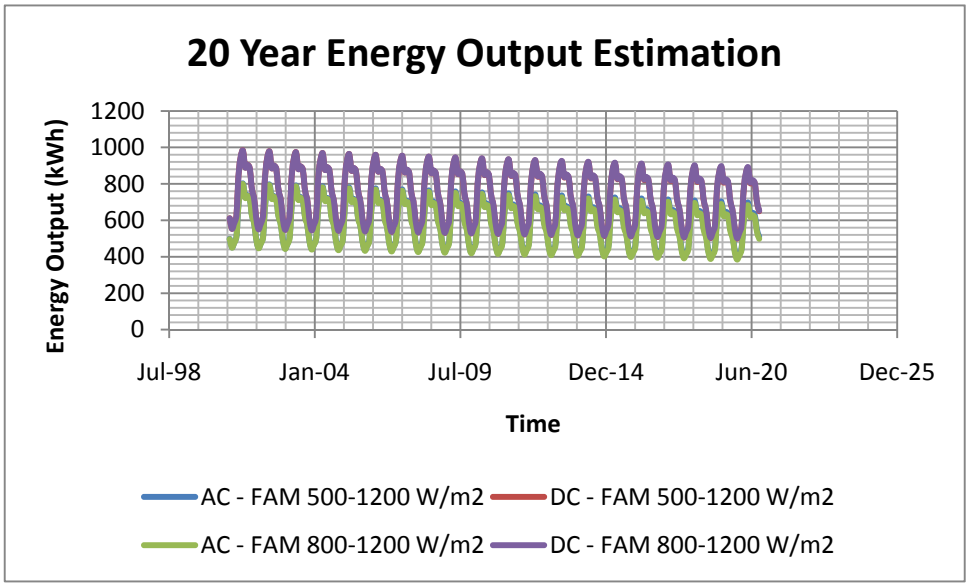

Figure 4-6 FAM Energy Output Prediction for 20 Years

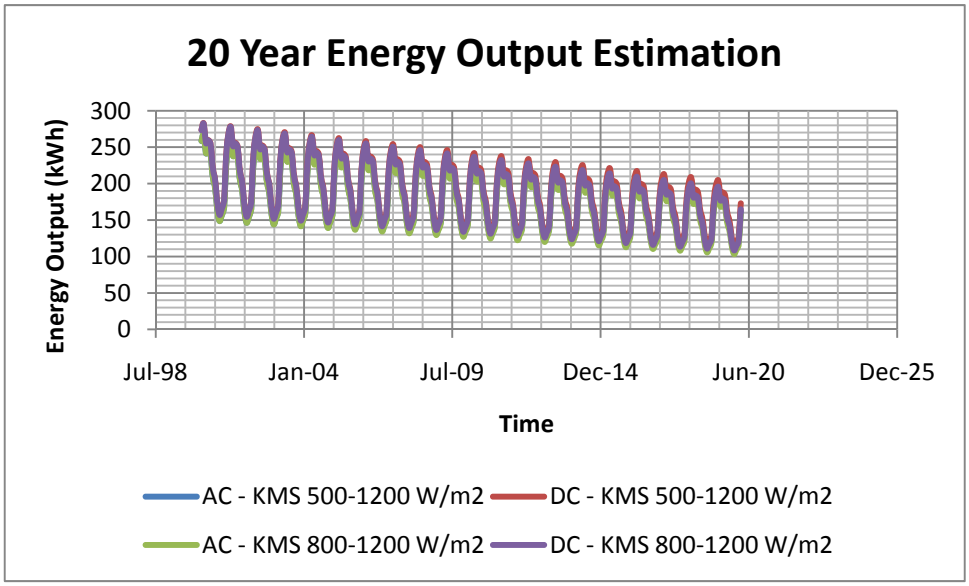

Figure 4-7 KMS Energy Output Prediction for 20 Years

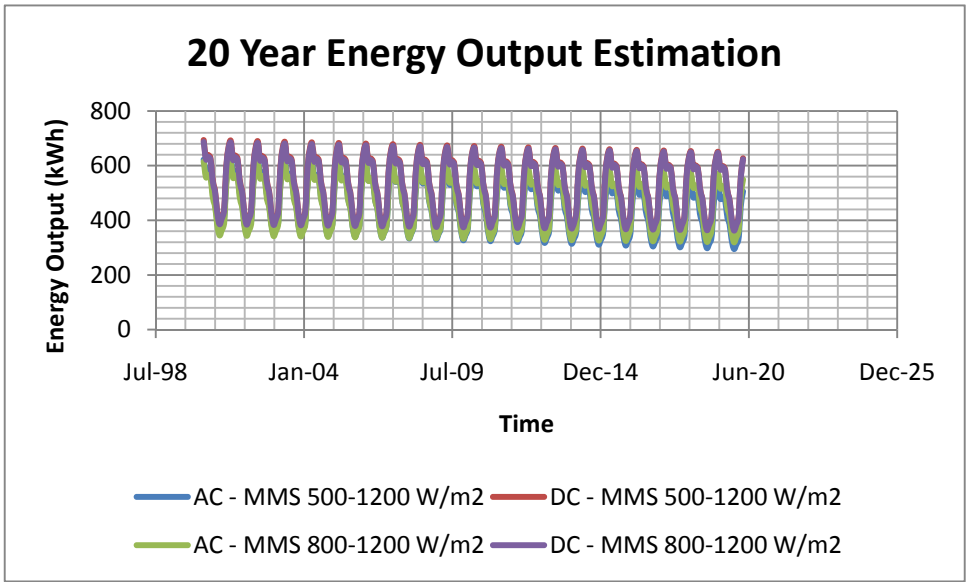

Figure 4-8 MMS Energy Output Prediction for 20 Years

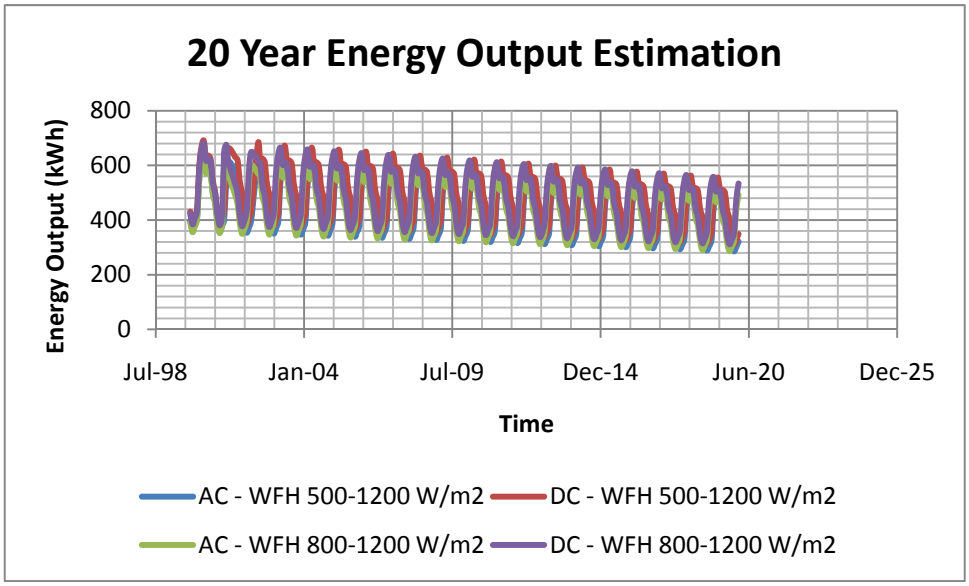

Figure 4-9 WFH Energy Output Prediction for 20 Years

4.5.1 Comparison of the PV Output

The plots shown below show the performance of each system and compare the obtained results by filtering the monthly data in two different ranges for the irradiation.

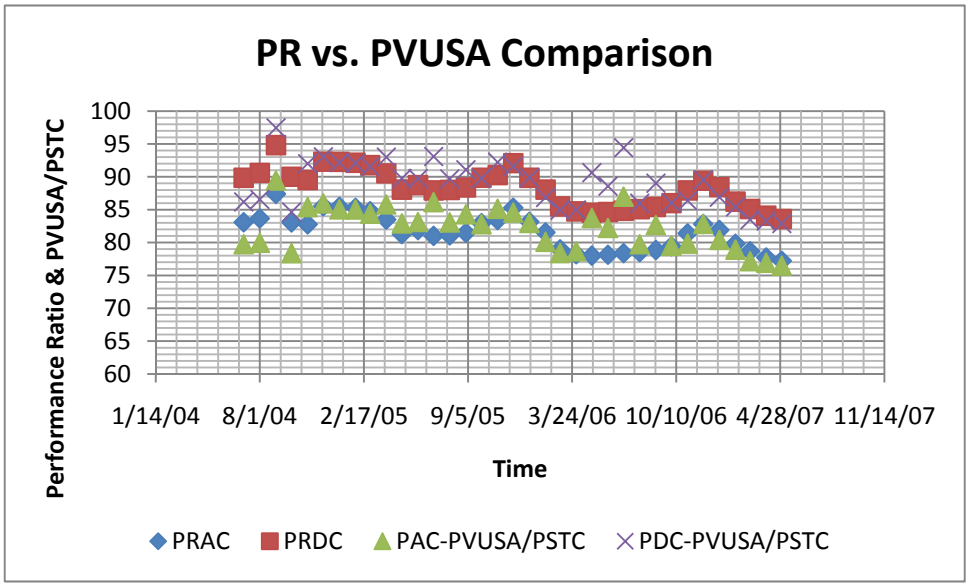

Figure 4-10 CEL Data Comparison (500-1200 W/m^2)

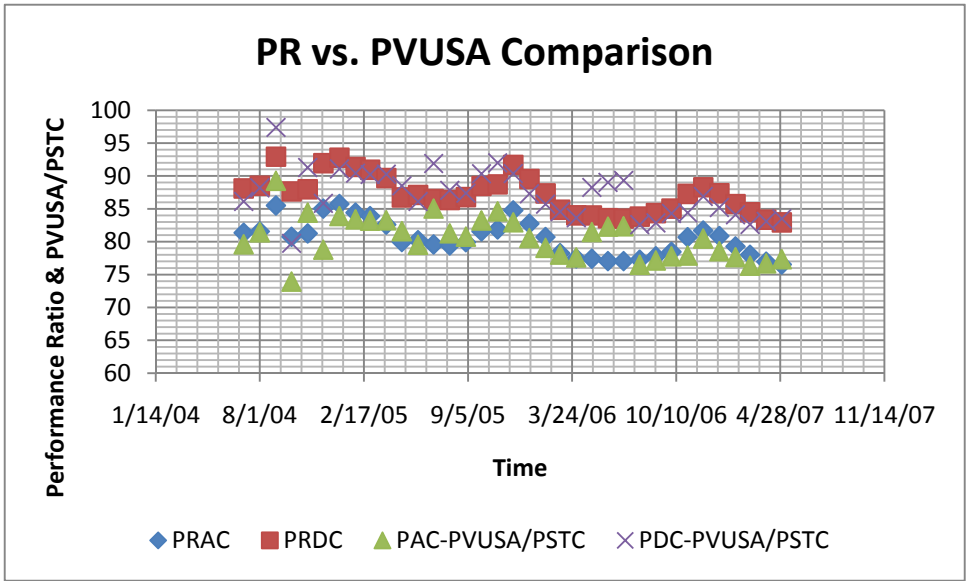

Figure 4-11 CEL Data Comparison (800-1200 W/m^2)

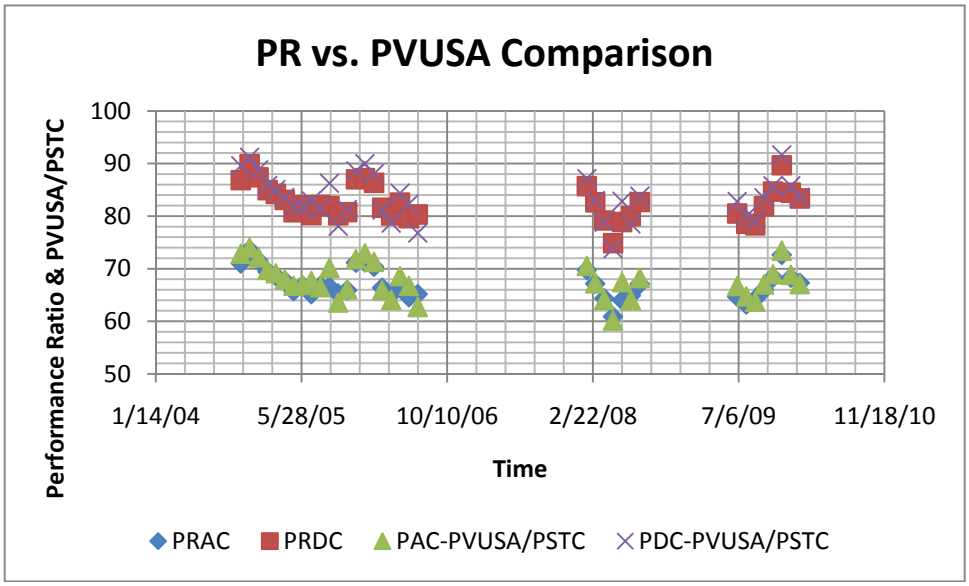

Figure 4-12 FAM Data Comparison (500-1200 W/m^2)

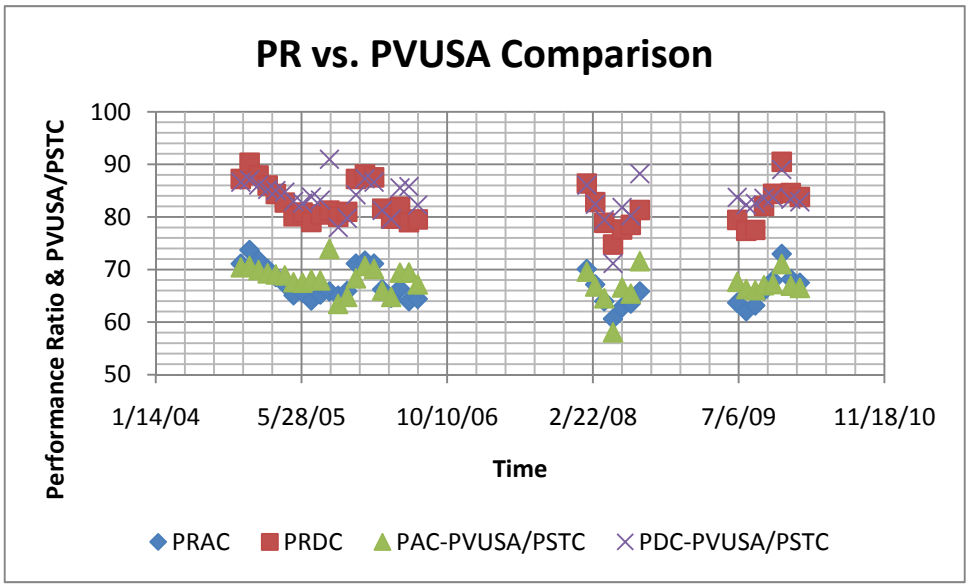

Figure 4-13 FAM Data Comparison (800-1200 W/m^2)

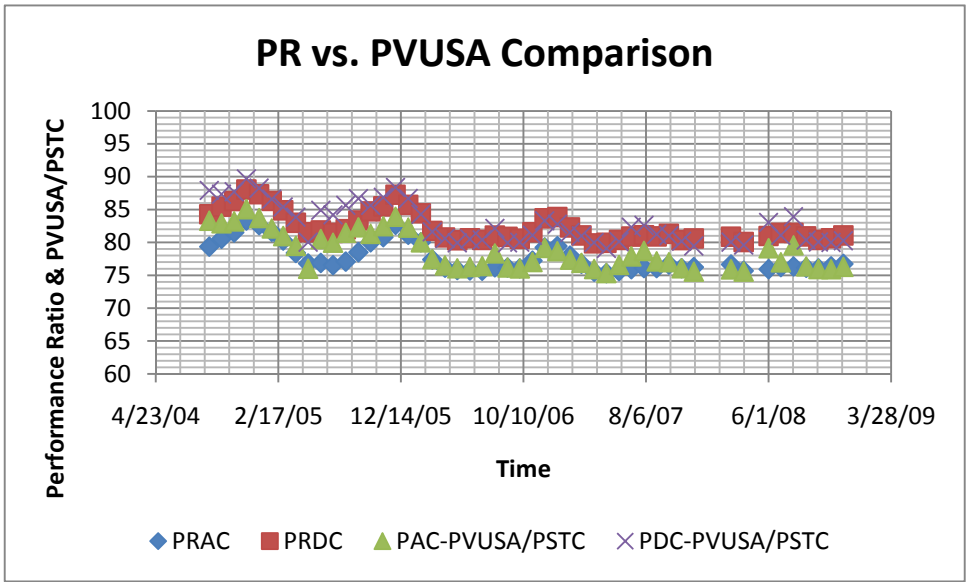

Figure 4-14 KMS Data Comparison (500-1200 W/m^2)

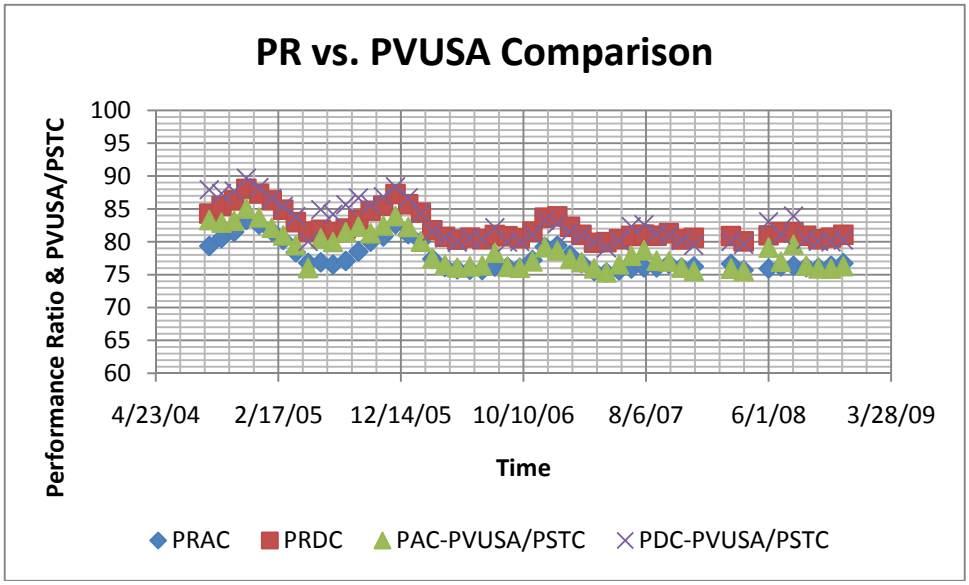

Figure 4-15 KMS Data Comparison (800-1200 W/m^2)

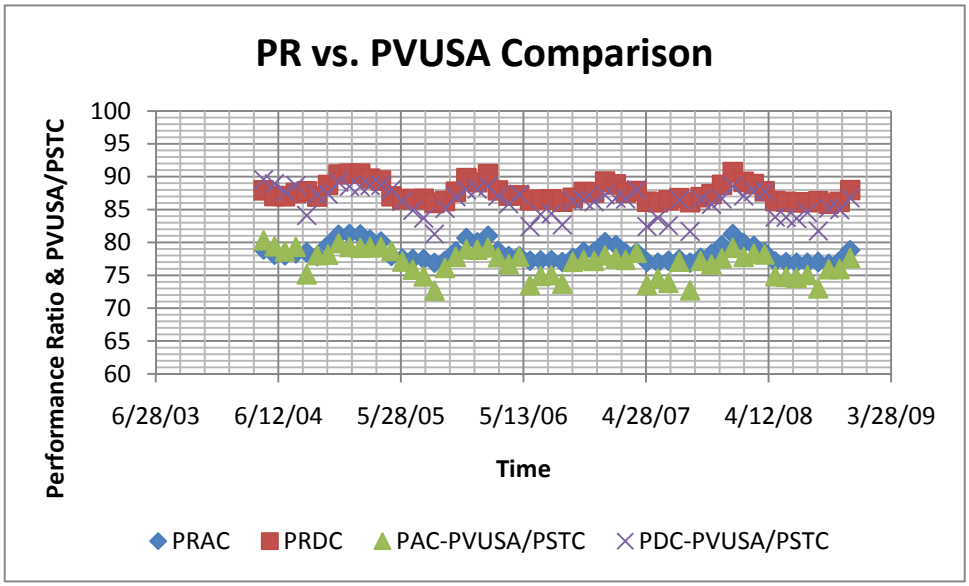

Figure 4-16 MMS Data Comparison (500-1200 W/m^2)

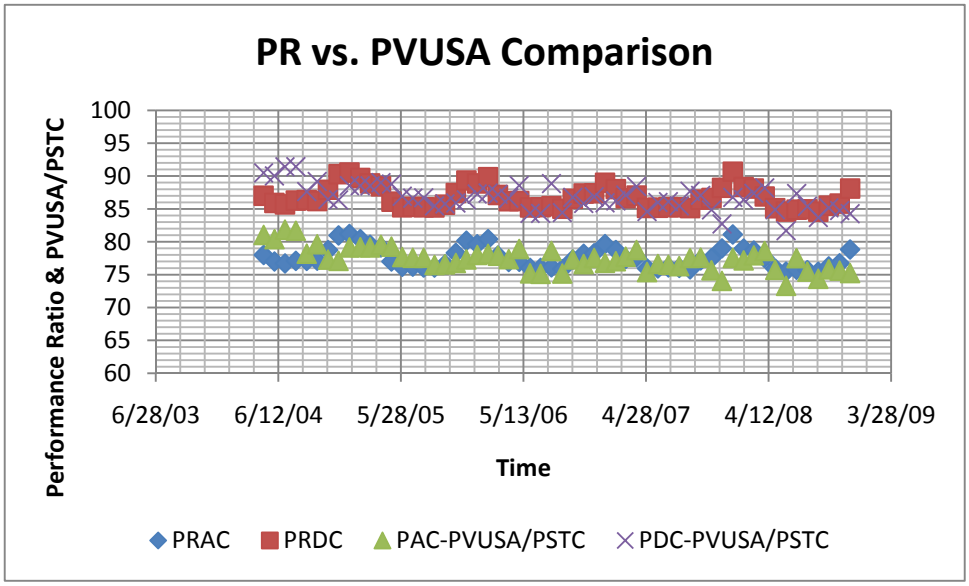

Figure 4-17 MMS Data Comparison (800-1200 W/m^2)

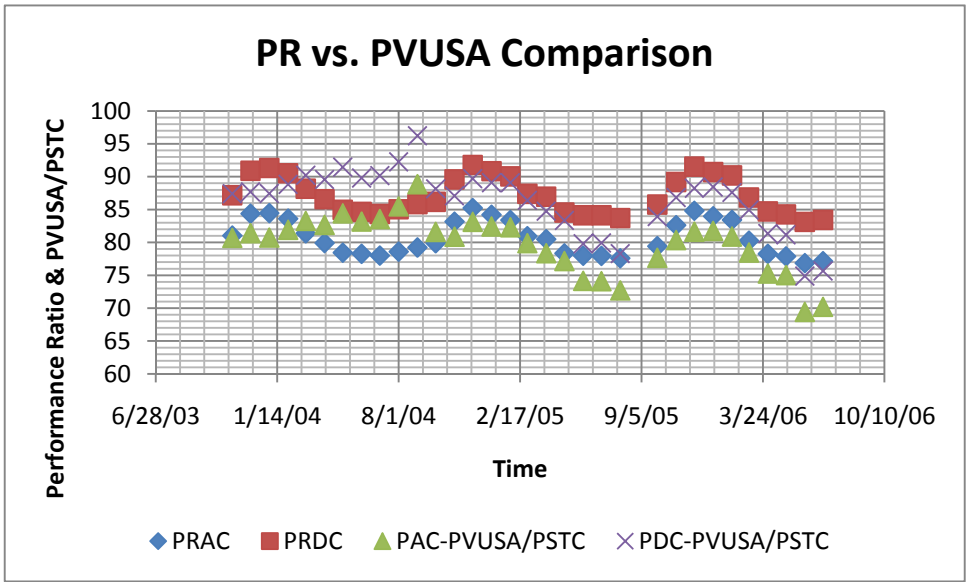

Figure 4-18 WFH Data Comparison (500-1200 W/m^2)

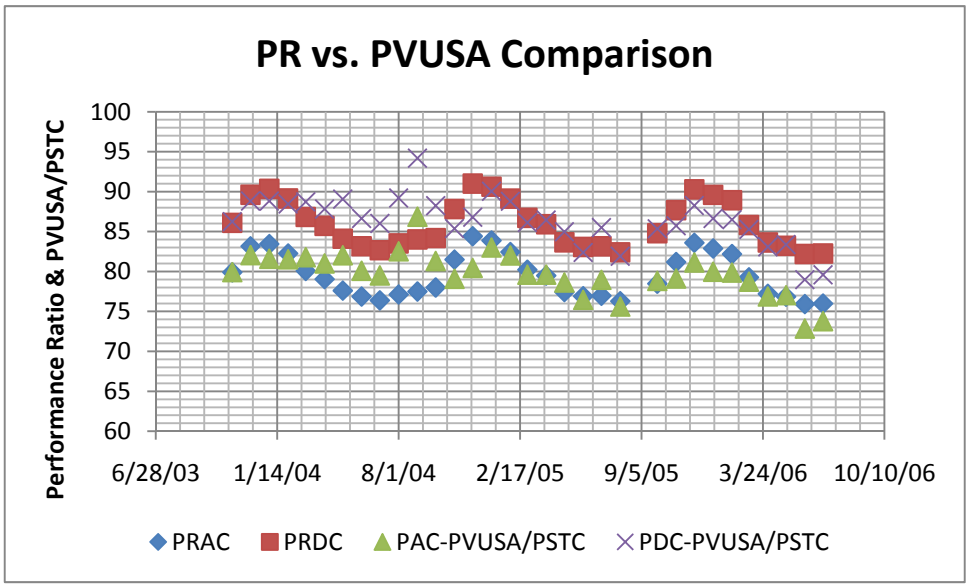

Figure 4-19 WFH Data Comparison (800-1200 W/m^2)

4.5.2 Uncertainty Estimation

The uncertainty in each variable is propagated through sensitivity coefficients, which are the partial derivatives of the right hand side of equation 2-9 with respect to each independent variable [26][27]. The following partial derivatives represent the sensitivity coefficients for the PVUSA regression equation shown in equation 2-9.

$$\frac{\delta P}{\delta I} = a + 2Ib + cW + dT \qquad (4\text{-}2)$$

$$\frac{\delta P}{\delta W} = cI \qquad (4\text{-}3)$$

$$\frac{\delta P}{\delta W} = dI \qquad (4\text{-}4)$$

Equation 4-4 Sensitivity Coefficient for Ambient Temperature, T

Instrumentation error contributes to measurement uncertainty and must be taken into consideration when calculating uncertainties in the measurements taken. These specifications are often constants that can be found on manufacturer specification sheets, and as shown in equation 4-5 below, e_I, e_W, and e_T, each correspond to instrumentation measurement error or uncertainty in each of the equipment that measures irradiance, wind speed, and ambient temperature respectively.

$$e_p = \sqrt{(\frac{\delta P}{\delta I} e_I)^2 + (\frac{\delta P}{\delta W} e_W)^2 + (\frac{\delta P}{\delta T} e_T)^2} \qquad (4\text{-}5)$$

Table 4-6 below shows the average total uncertainty calculated in the PVUSA Regression analysis performed on the five systems studied in both, 500-1200 W/m^2 and 800-1200 W/m^2 ranges as well as on the AC side and DC side of each system.

Table 4-6 Average Total Uncertainty in PVUSA Regression Uncertainty

System	PVUSA AC (500 – 1200 W/m²)	PVUSA DC (500 – 1200 W/m²)	PVUSA AC (800 – 1200 W/m²)	PVUSA DC (800 – 1200 W/m²)
CEL	±153.51 W	±167.54 W	±139.29 W	±153.48 W
FAM	±200.36 W	±252.61 W	±180.96 W	±229.71 W
KMS	±67.240 W	±68.971 W	±63.510 W	±65.802 W
MMS	±142.19 W	±161.00 W	±139.77 W	±159.96 W
WFH	±146.93 W	±159.96 W	±143.71 W	±158.45 W

4.6 Real Time Data Comparison

The CEL and MMS system are identical systems differing only on installation location. After doing the Performance Ratio and the PVUSA Regression analysis it was notable the difference in degradation rates per year on both systems. The CEL system degraded at an average rate of 2.34% per year while the MMS system degraded at an average rate of 0.94% per year. Therefore, a site visit was necessary to understand why this happened. Visiting the CEL system and taking a few I-V measurements resulted in noticing that the pyranometer installed was not calibrated therefore resulting in observed higher degradation rates when the different analyses were performed. Figure 4-25 represents the relative difference of the data measured the day of the site visit against the data recorded over time. It is clearly seen how the degradation rate is much lower when calibrated sensors are used to measure data.

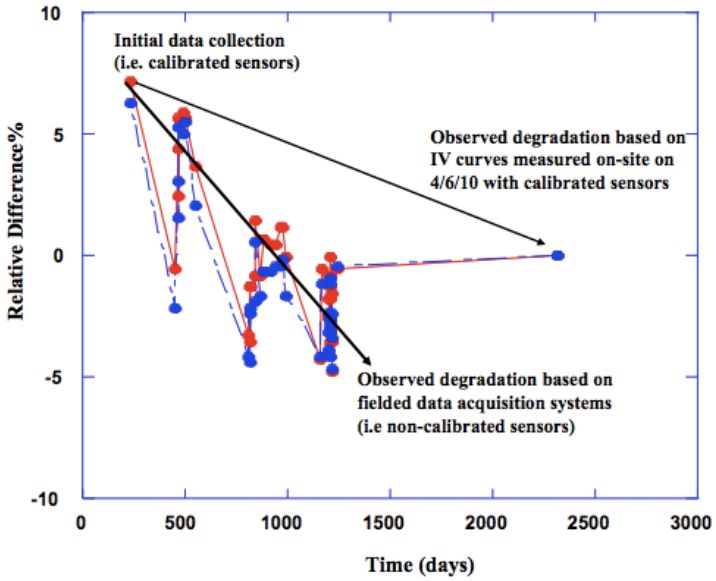

Figure 4-20 Observed Degradation (DAS vs. IV Curves on Site)

4.7 Theoretical and Experimental Performance and Solar Illumination Assessments as Functions of the Angle of Incidence in Florida

As mentioned before, NREL in conjunction with SNL and the DOE have developed SAM, which allows to examine energy production and lets the user compare field measured PV output with theoretical data on a typical meteorological year for a given location, orientation and installation angle.

4.7.1 Experimental Setup

To verify the SAM model, three types of PV modules (Single-Crystal Silicon, Multi-Crystalline Silicon, and Amorphous Silicon) have been investigated experimentally under actual field conditions in Florida for more than one year. The modules were mounted at several different tilt angles between 28° and 35° with respect to the horizon. The current-

voltage (I-V) and power-voltage (P-V) characteristics of the different modules were measured under different meteorological conditions.

Solar irradiance measurements were made using pyranometers installed in the same plane as the modules. Temperature measurements were made using thermocouples configured to measure ambient temperature and module temperature. Finally other sensors were used to measure DC voltage and current from the array, along with sensors to collect AC data from the inverter.

4.7.2 Results and Discussions

Various photovoltaic modules have been integrated into buildings in different places in Florida and have been monitored by FSEC. During a typical year, the temperature of the photovoltaic arrays can vary from -13° to over 75° and the solar irradiance varies from 0 W/m^2 to 1300 W/m^2. As various photovoltaic modules respond differently to each of these parameters, it is not surprising that the relative performance of photovoltaic modules exposed to actual operating conditions does not duplicate that obtained at a fixed set of rating conditions [28].

4.7.3 Radiation Characteristics

The availability of solar radiation for technological applications is determined by the clearness of the sky. Figure 4-21 below shows the average solar irradiation for the reference point (Daytona Beach) and three other sites where data was measured over the period of one year. It is clearly shown how the peak and the lowest months on the measured data are April and December respectively.

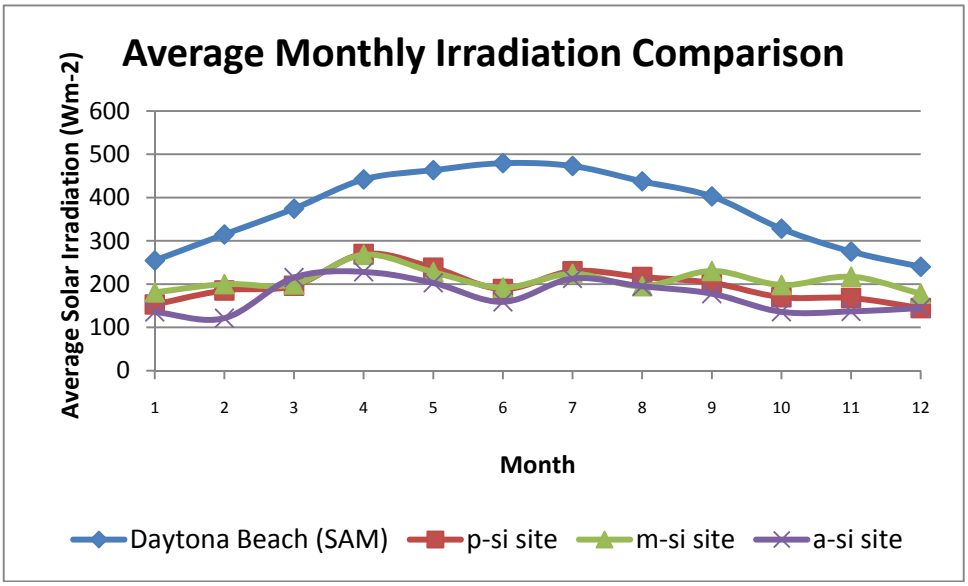

Figure 4-21 Average Monthly Irradiation Comparison

4.7.4 Power Output and Tilt Angle

The power incident on a PV module depends not only on the power contained in the sunlight, but also on the angle between the module and the sun. When the absorbing surface and the sunlight are perpendicular to each other, the power density on the surface is equal to that of the sunlight. However, as the angle between the sun and a fixed surface is continually changing, the power density on a fixed PV module is less than that of the incident sunlight. The tilt angle of a PV array affects the amount of power output and incident light a system is exposed to. SAM was used to estimate the monthly AC power output of the tilted PV surface, and to determine optimum tilt angles for PV panels installed in Florida (Daytona Beach used as reference w/ Sharp NE-Q5E2U 1.5kW system and SMA America SB3000US 240V inverter). Figure 4-22 shows the above mentioned.

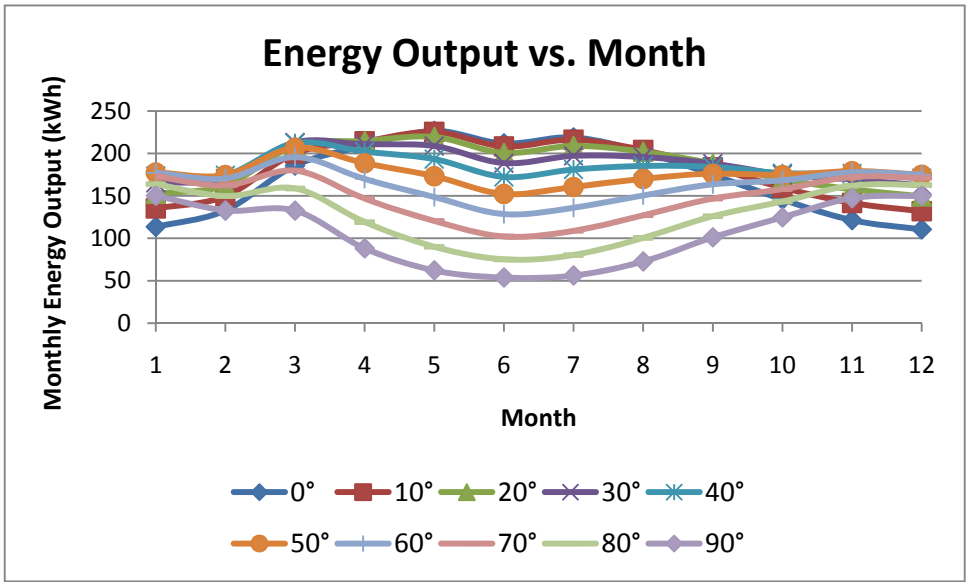

Figure 4-22 Monthly Energy Output as a Function of Time and Tilt Angle

Figure 4-23 illustrates the relationship between tilt angle and the yearly AC power output for three different technologies (Single-Crystal Silicon; Siemens SP-150, Multi-Crystalline Silicon; Sharp NE-Q5E2U, and Amorphous Silicon; Uni-Solar SHR-17). Reference point for this comparison was Daytona Beach with 1.5kW systems oriented 180 South and connected to SMA America SB3000US 240V inverters. The reason for the difference in the AC Power Outputs for the three systems is because of how cell temperature and other factors affect the power output of each system.

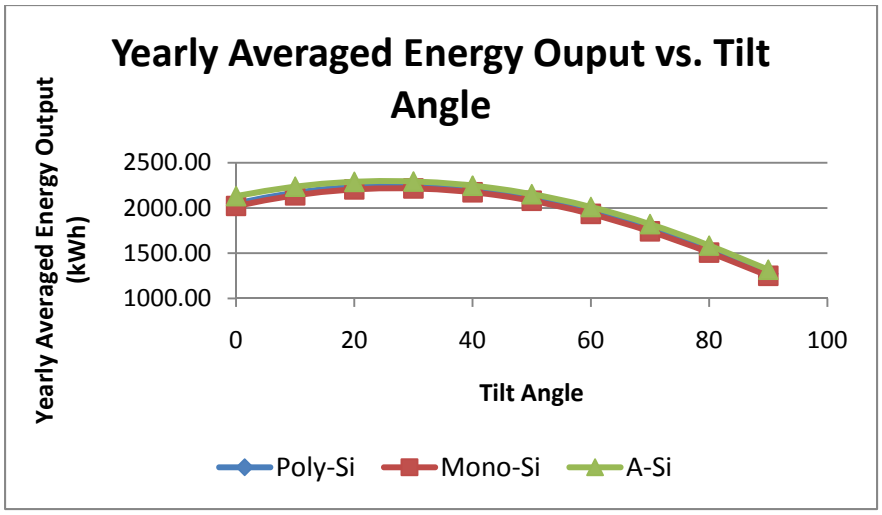

Figure 4-23 Energy Output as a Function of Tilt Angle

The optimum tilt angles were determined by searching for the values of angles for which the yearly AC Power Output was a maximum. According to the power output calculations, the optimal tilt angle for the whole year is around 27° and can be modeled by the following equation for this particular set of systems by averaging all three systems output and performing a curve fit:

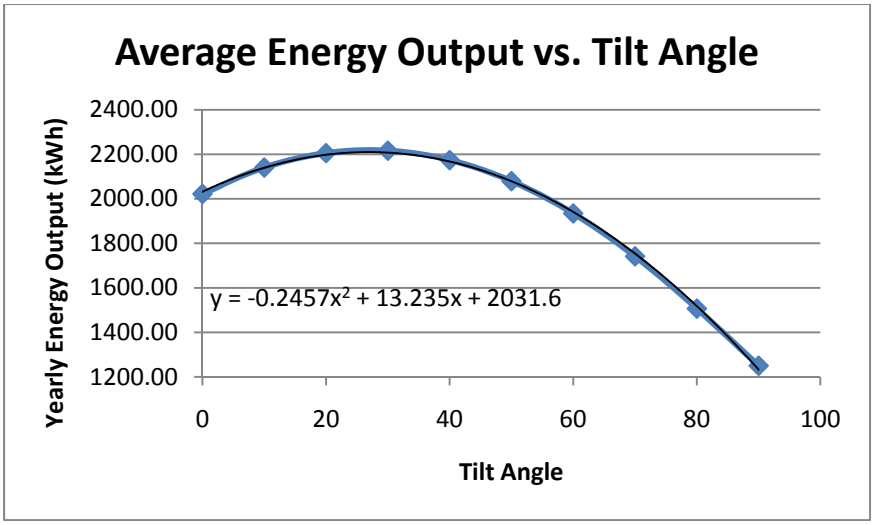

Figure 4-24 Average Energy Output as a Function of Tilt Angle

$$P(\theta) = -0.2457\theta^2 + 13.235\theta + 2031.6 \qquad (4\text{-}6)$$

If the derivative of P_{AC} is calculated and evaluated at zero, the angle at which maximum power is drawn out of the arrays can be calculated. Therefore,

$$\frac{dP_{AC}(\theta)}{d\theta} = -0.4914\theta + 13.235 \qquad (4\text{-}7)$$

and it is calculated that the maximum power is drawn when θ = 27°.

4.7.5 Measured and Simulated Monthly Averaged AC Power Output

Figure 4-25 shows the comparison between measured and simulated monthly averaged AC output power of the three different technologies mentioned before. After this analysis is done, it is found that the simulated and measured results have the same trend with an average relative difference of 16.28%. The monthly power output of PV modules has a similar tendency as the radiation intensity, and in general the power output per solar cell area should have an approximate linear relationship with the radiation intensity. Moreover, weather conditions also have an influence on the conversion efficiency of the PV System. Higher conversion efficiency of the PV system can be obtained with the clearness of the weather but also the conversion efficiency of the PV system should fall more rapidly than the decrease of slope radiation in bad weather conditions.

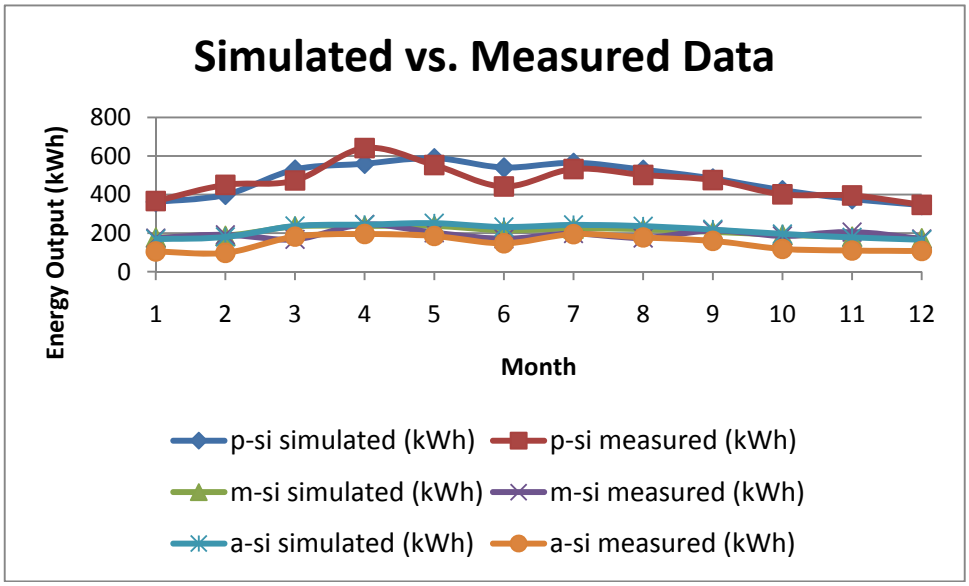

Figure 4-25 Simulated Data vs. Measured Data on a Given Year

CHAPTER 5 CONCLUSIONS AND DISCUSSIONS

In this study, accurate measurements of data were collected from five individual PV systems installed in the state of Florida, with the purpose of studying their degradation rates. Such data was collected utilizing highly calibrated instruments that measured voltage, current, power, solar irradiation, and temperature every second and averaging it every fifteen minutes.

Currently about eighty-six percent of PV manufacturers produce crystalline technologies making it imperative to study how this type of technology behaves when exposed in the field. Performing the analysis of five PV systems installed in Florida and monitored by the Florida Solar Energy Center led to a better understanding of the performance and degradation rates experienced by field aged PV arrays. This analysis, performed by applying two different techniques is expressed in performance ratio and power rate, and results are shown in Tables 5-1 and 5-2.

Table 5-1 Results for 500-1200 W/m^2

System	Array Degradation (DC) / year		Estimated DC Energy Production (20 years)	Array Degradation (AC) / year		Estimated AC Energy Production (20 Years)
	PR	PVUSA		PR	PVUSA	
CEL	-2.73%	-2.34%	293.11 kWh	-2.69%	-2.31%	275.64 kWh
FAM	-0.57%	-0.48%	649.42 kWh	-0.68%	-0.69%	509.80 kWh
KMS	-1.44%	-1.96%	172.91 kWh	-1.46%	-1.93%	162.00 kWh
MMS	-0.33%	-0.75%	626.74 kWh	-0.40%	-0.82%	505.74 kWh
WFH	-1.07%	-4.40%	348.71 kWh	-1.08%	-4.34%	321.73 kWh

Table 5-2 Results for 800-1200 W/m^2

System	Array Degradation (DC) / year		Estimated DC Energy Production (20 years)	Array Degradation (AC) / year		Estimated AC Energy Production (20 Years)
	PR	PVUSA		PR	PVUSA	
CEL	-2.49%	-2.39%	320.92 kWh	-2.42%	-2.29%	303.38 kWh
FAM	-0.57%	-0.39%	652.80 kWh	-0.76%	-0.62%	498.79 kWh
KMS	-1.60%	-2.18%	164.82 kWh	-1.57%	-2.16%	156.96 kWh
MMS	-0.31%	-1.01%	622.98 kWh	-0.38%	-1.10%	549.41 kWh
WFH	-1.02%	-2.30%	533.55 kWh	-1.03%	-2.31%	491.86 kWh

Previous studies performed by Sandia have shown losses on open-circuited modules of about 0.5% per year while NREL reports degradation of about 0.7% year [35]. Having this in mind leads to various conclusions, which in fact results in obvious calibration problems on some of the systems. Instrument calibration, such as the pyranometer, is of the key for this experiment, which is the primary reason why these two systems show higher degradation rates than the other calibrated systems. Pyranometer error is the typical cause of the observed high degradation rates. This means constant monitoring and calibration of pyranamoters should be done to ensure readings are accurate.

Different factors cause degradation and module failure when exposed in the field. Typical degradation is often a result of factors such as [36]:

- degradation of packaging materials
- loss of adhesion of encapsulants
- degradation of cell/module interconnection
- degradation caused by moisture intrusion
- degradation of the semiconductor device

Filtering of data in two different ranges of irradiation showed no difference in the degradation rates calculated. An average difference of 0.02% is observed in the performance ratio analysis while 0.33% is observed in the PVUSA analysis. This is clear evidence that as long as the collected data is clean, the amount of data used per month does not affect the result, although using a larger window of data is better when performing regressions over long periods of time.

These two methods use two unique approaches to calculate PV performance. On one hand, the performance ratio analysis uses only the incident irradiation and the output power to determine performance, while the PVUSA analysis considers other factors such as wind speed and ambient temperature along with incident irradiance. The PVUSA analysis should be a better method when used in conjunction with calibrated instruments, because it takes into account more degradation parameters.

The analysis of the five PV systems studied led also to a better understanding of seasonal variations, where it was found and confirmed the typical output increase during the colder months, as it would be expected for crystalline technologies. As shown in the collected data, the performance ratio analysis clearly shows the variation in performance depending on the different seasons of the year as well as the PVUSA regression analysis.

On the other hand, on a performance and solar illumination assessment and evaluation, three PV systems installed in Florida were used in order to validate the Solar Advisor Model (SAM). By analyzing the measured and calculated data, the solar radiation, the relationship between the tilt angles, and AC power output were investigated. Based on the results, it can be found that the power output of a PV module has a strong relationship

with the tilt angle and solar radiation. The Solar Advisor Model was used, and the calculated values were verified and compared with the measured values. According to the information found, the optimal tilt angle for the whole year in Florida is around 27° in Florida.

With current site visits there is plenty of room to expand this project. I-V curve measurements with calibrated instruments can be taken at all of the selected systems and trace current measurements with newly onsite measurements and calculate their relative difference to compare results as it was done on the CEL system and as shown in section 4.6. Irradiance data from nearby calibrated weather stations can also be compared with system data and calculate how much it has drifted. Doing that could help obtain better degradation results since pyranomter calibration seems to be the principal cause of high degradation rates. Other work also include the possibility of reactivating many of the data loggers and start collecting data once more to keep studying the long-term degradation of these field-aged systems. Table 3-1 shows a list of systems also monitored by FSEC that could be used for future analyses of the same type as presented in this thesis.

APPENDIX
COMPUTER PROGRAMS

MATLAB: PVUSA & Performance Ratio Calculator

```
function dummy = degradation()
format short;
disp(' ');
file_name = input('Enter File Name: ', 's');
output_name = input('Enter Output File Name: ', 's');
power_array_stc = input('Enter System Power (STC): ');
power_system_stc = input('Enter Total System Power (STC): ');
irradiance_stc = input('Enter Irradiance at STC(Usually 1000): ');
ambient_temperature_range_prompt = input('Enter Column Where Ambient Temperature
is: ', 's');
irradiance_range_prompt = input('Enter Column Where Irradiance is: ', 's');
ac_power_1_prompt = input('Enter Column Where AC Power 1 is: ', 's');
ac_power_2_prompt = input('Enter Column Where AC Power 2 is: ', 's');
dc_power_1_prompt = input('Enter Column Where DC Power 1 is: ', 's');
dc_power_2_prompt = input('Enter Column Where DC Power 2 is: ', 's');
[type, excel_tab] = xlsfinfo(file_name);
disp(' ');
disp('Calculating Data for:');
size_of_array_tab = size(excel_tab);
output_size = zeros(size_of_array_tab(2),1);
date_output = output_size;
```

```
pr_ac_output = output_size;
a_ac_output = output_size;
b_ac_output = output_size;
d_ac_output = output_size;
pvusa_ac_output = output_size;
pr_dc_output = output_size;
a_dc_output = output_size;
b_dc_output = output_size;
d_dc_output = output_size;
pvusa_dc_output = output_size;
for i=1:size_of_array_tab(2),
   disp(char(excel_tab(i)));
   irradiation = xlsread(file_name,char(excel_tab(i)),irradiance_range_prompt);
   ambient_temperature =
   xlsread(file_name,char(excel_tab(i)),ambient_temperature_range_prompt);
   %AC DATA
   ac_power_1 = xlsread(file_name,char(excel_tab(i)),ac_power_1_prompt);
   ac_power_2 = xlsread(file_name,char(excel_tab(i)),ac_power_2_prompt);
   ac_power = ac_power_1 + ac_power_2;
   ac_power_over_irradiation = ac_power./irradiation;
   predictors_ac = [ones(size(ac_power)) irradiation ambient_temperature];
```

```
response_ac = predictors_ac\ac_power_over_irradiation;
ac_1_yf = (ac_power_1*0.25)./power_array_stc;
ac_2_yf = (ac_power_2*0.25)./power_array_stc;
ac_yf = sum(ac_1_yf + ac_2_yf);
ac_1_yr = (irradiation*0.25)./irradiance_stc;
ac_2_yr = (irradiation*0.25)./irradiance_stc;
ac_yr = sum(ac_1_yr + ac_2_yr);
ac_pr = ac_yf/ac_yr;
ac_pvusa = 1000*(response_ac(1)+1000*response_ac(2)+20*response_ac(3));
%DC DATA
dc_power_1 = xlsread(file_name,char(excel_tab(i)),dc_power_1_prompt);
dc_power_2 = xlsread(file_name,char(excel_tab(i)),dc_power_2_prompt);
dc_power = dc_power_1 + dc_power_2;
dc_power_over_irradiation = dc_power./irradiation;
predictors_dc = [ones(size(dc_power)) irradiation ambient_temperature];
response_dc = predictors_dc\dc_power_over_irradiation;
dc_1_yf = (dc_power_1*0.25)./power_array_stc;
dc_2_yf = (dc_power_2*0.25)./power_array_stc;
dc_yf = sum(dc_1_yf + dc_2_yf);
dc_1_yr = (irradiation*0.25)./irradiance_stc;
dc_2_yr = (irradiation*0.25)./irradiance_stc;
dc_yr = sum(dc_1_yr + dc_2_yr);
```

```
    dc_pr = dc_yf/dc_yr;
    dc_pvusa = 1000*(response_dc(1)+1000*response_dc(2)+20*response_dc(3));
    %date_output(i,1) = chaexcel_tab(i);
    pr_ac_output(i,1) = ac_pr;
    a_ac_output(i,1) = response_ac(1);
    b_ac_output(i,1) = response_ac(2);
    d_ac_output(i,1) = response_ac(3);
    pvusa_ac_output(i,1) = ac_pvusa;
    pr_dc_output(i,1) = dc_pr;
    a_dc_output(i,1) = response_dc(1);
    b_dc_output(i,1) = response_dc(2);
    d_dc_output(i,1) = response_dc(3);
    pvusa_dc_output(i,1) = dc_pvusa;
end
data =
[pr_ac_output,a_ac_output,b_ac_output,d_ac_output,pvusa_ac_output,pr_dc_output,a_dc_out
put,b_dc_output,d_dc_output,pvusa_dc_output];
disp(data);
xlswrite(output_name, data);
```

REFERENCES

[1] King, D. L., Boyson, W. E., and Kratochvil, J. A. (2002). Analysis of factors influencing the annual energy production of photovoltaic systems. Proceedings of the 29th IEEE Photovoltaic Specialists Conference, 1356-1361

[2] Marion, B. (2002). A method for modeling the current-voltage curve of a PV module for outdoor conditions *Progress in photovoltaics: research and applications, 10,* 205-214.

[3] Masters, G. M. (2004*). Renewable and efficient electric power systems*. New York: John Wiley and Sons.

[4] Dunlop, J. (2010). *Photovoltaic systems*. Orland Park, Illinois: American Technical Publishers.

[5] UO solar radiation monitoring laboratory. Retrieved from University of Oregon. Website: http://solardat.uoregon.edu/.

[6] Crystalline silicon terrestrial photovoltaic (PV) modules – Design qualification and type approval (2005). Geneva, Switzerland: International Electrotechnical Comission.

[7] Thin-film terrestrial photovoltaic (PV) modules – Design qualification and type approval (2008). Geneva, Switzerland: International Electrotechnical Comission.

[8] King, D.L., Kratochvil, J.A., Boyson W.E. (1997). *Temperature coefficients for PV modules and arrays: measurement methods, difficulties, and results*. Presented at the 26th IEEE Photovoltaic Specialists Conference, Anaheim California.

[9] Whitaker, C.M., Townsend, T.U., Wenger, H.J., Iliceto, A, Chimento, G., Paletta, F. (1991). Effects of irradiance and other factors on PV temperature coefficients.

[10] King. D.L., Kratochvil, J.A., Boyson, W.E. (n.d.). Stabilization and performance characteristics of commercial amorphous-silicon PV modules.

[11] Akhmad, K., Kitamura, A., Yamamoto, F., Okamoto, H., Takakura, H., Hamakawa, Y., (1996). Outdoor performance of amorphous silicon and polycrystalline silicon PV modules.

[12] Ruther, R., Tamizh-Mani, G., del Cueto, J., Adelstein, J., Montenegro, A.A., von Roedern, B. (n.d.). Performance test of amorphous silicon modules in different climates: higher minimum operating temperatures lead to higher performance levels.

[13] Del Cueto, J.A. (2002, May) Comparison of energy production and performance from flat-plate photovoltaic module technologies deployed at fixed tilt. Presented at the 29th IEEE Photovoltaic Specialists Conference, New Orleans.

[14] Meike, W. (1998). Hot climate performance comparison between poly-crystalline and amorphous silicon cells connected to an utility mini-grid. Presented at Solar '98, Christchurch, NZ.

[15] Kroposki, B., Emery, K., Myers, D., Mrig, L. (1994, December). A comparison of photovoltaic module performance evaluation methodologies for energy ratings.

[16] Kroposki, B., Myers, D., Emery, K., Mrig, L., Whitaker, C., Newmiller, J. (1996, May) Photovoltaic module energy rating methodology development.

[17] Kroposki, B., Mrig., L., Whitaker, C., Newmiller., J. (1995, May). Development of a photovoltaic module energy ratings methodology. Presented at the 13th NREL PV Program Review Meeting, Lakewood, Colorado.

[18] Marion, B., Adelstein, J., Boyle, K., Hayden, H., Hammond, B., Fletcher, T., Canada, B.,

Shugar, D., Wenger, H., Kimber, A., Mitchell, L., Rich, G., Townsend, T. (2005, January). Performance parameters for frid-connected PV systems. Prepared for the 31st IEEE Photovoltaics Specialist Conference and Exhibition, Lake Buena Vista, FL.

[19] Myers, D. (2009, May). Evaluation of the performance of the PVUSA rating methodology applied to DUAL junction PV technology. Presented at the American Solar Energy Society Annual Conference, Buffalo, NY.

[20] NREL: Solar Advisor Model (SAM): Background. Retrieved from National Renewable Energy Laboratory. Website:https://www.nrel.gov/analysis/sam/background.html

[21] Azab, M. (2009). Improved circuit model of photovoltaic array. International Journal of Electrical Power and Energy Systems Engineering.

[22] Makrides, G., Zinsser, B., Georghiou, G.E., Werner, J. (n.d.). Performance assessment of different photovoltaic systems under identical field conditions of high irradiation.

[23] Whitaker, C.M., Townsend, T.U., Newmiller, J.D., King, D.L., Boyson, W.E., Kratochvil, J.A., Collier, D.E., Osborn, D.E. (1997, September). Application and validation of a new PV performance characterization method. Presented at the 26th IEEE Photovoltaic Specialists Conference, Anaheim, CA.

[24] Photovoltaic Modules. Retrieved from Florida Solar Energy Center. Website: http://www.fsec.ucf.edu/en/industry/testing/PVmodules/index.htm

[25] Photovoltaics. Retrieved from Florida Solar Energy Center. Website: http://www.fsec.ucf.edu/en/research/photovoltaics/index.htm

[26] Evaluation of measurement data - guide to the expression of uncertainty in

measurement. (2008, September) Published by OSOTAG 4, 1995. International Bureau of Weights and Measures (BIPM) Sevres, France.

[27] Taylor, B.N., C E Kuyatt. (1994). Guidelines for Evaluation and Expressing the Uncertainty of NIST Measurement Results. NIST Technical Note 1297. National Institute of Standards and Technology.

[28] Fanney, A.H., Dougherty, B.P., and Davis, M.W. (2002, May). Performance and characterization of building integrated photovoltaic panels. Proceedings of the 29th IEEE Photovoltaic Specialist Conference, (CD-ROM) New Orleans, LA.

[29] De Miguel, A., Bilbao, J., Cazorro, J.R.S., Martín, C. (n.d.). Performance analysis of a grid-connected PV system in a rural site in the northwest of Spain. Department of Applied Physics I. Faculty of Science. University of Valladolid (Spain).

[30] Davis, K., Moaveni, H., (n.d.). Effects of module performance and long-term degradation on economics and energy payback: Case study of two different photovoltaic technologies.

[31] NREL: Performance and Reliability R&D – Indoor Testing. Retrieved from National Renewable Energy Laboratory. Website: http://www.nrel.gov/pv/performance_reliability/ indoor_testing.html

[32] Photovoltaic Electrical Power Systems Inspector/Installer Checklist. (2005). National Electric Code Article 690.

[33] Mah, O. (1998) Fundamentals of Photovoltaic Materials. National Solar Power Research Institute, Inc.

[34] Current status and progress in the new generation's silicon based solar cells. Retrieved

from Posterus. Website: http://www.posterus.sk/?p=1247

[35] Quintana, M.A., King, D.L., McMahon, T.J., Osterwald, C.R. (n.d.). Commonly observed degradation in field-aged photovoltaic modules.

[36] Vazquez, M. Rey-Stolle, I. (2008). Photovoltaic module reliability model based on field degradation studies.

[37] Technology fundamentals: The sun as an energy resource. Website: http://www.volker-quaschning.de/articles/fundamentals1/index.php